Pergamon

Geochimica et Cosmochimica Acta, Vol. 66, No. 16, pp. 2959–2979, 2002

0016-7037/02 $22.00 + .00

PII S0016-7037(02)00885-2

A plagioclase–olivine–spinel–magnetite inclusion from Maralinga (CK): Evidence for sequential condensation and solid–gas exchange

GERO KURAT,[1,*] ERNST ZINNER[2] and FRANZ BRANDSTÄTTER[1]

[1]Naturhistorisches Museum, Postfach 417, A-1014 Vienna, Austria
[2]McDonnell Center for the Space Sciences and the Physics Department, Washington University, St. Louis, MO 63130, USA

(*Received September* 4, 2001; *accepted in revised form February* 27, 2002)

Abstract—We report a detailed petrography, mineral chemistry, and trace element study of MaTroc, a large calcium–aluminum-rich inclusion (CAI) (5 × 2.5 mm) of irregular triangular shape. The inclusion has a zonal structure: The core consists of a porous plagioclase–olivine–Ca-rich pyroxene intergrowth with subordinate apatite. Its texture is meta-gabbro-like, similar to other plagioclase–olivine inclusions (POIs). The mantle has variable thickness (0.1–1.5 mm) and consists of a compact symplectitic intergrowth of spinel (hercynite) and plagioclase with abundant dispersed magnetite, subordinate Ca-rich pyroxene, and traces of sulfides. The thin (5–50 μm) discontinuous crust of MaTroc consists mainly of plagioclase with some olivine and magnetite.

The Mg-Fe phases of MaTroc are Fe-rich: olivine has Fa33.2 and high NiO content, similar to that in the host rock, Ca-rich pyroxene has much lower TiO_2 and Cr_2O_3 contents than that of the host chondrite, and plagioclase is An55–An74. Magnetites have variable compositions, are poorer in Al_2O_3 and Cr_2O_3 and richer in NiO than those in the host. Spinels have also variable compositions, rich in FeO, NiO, and ZnO.

Despite their different mineralogy, both core and mantle have bulk trace element abundances similar to those in average group II CAIs. However, the mantle is richer in Nb and U and poorer in Eu, Be, B, Sr, and Li than the core. All minerals have high trace element contents. Minerals in the core show signs of incomplete equilibration of trace elements within and between them. Mantle minerals are far from equilibrium with each other and the bulk system. Spinel and anorthite carry the trace element signature of their precursor melilite (or hibonite), and magnetite contains large amounts of a heterogeneously distributed remnant extremely rich in trace elements ("obscurite"), possibly of a former perovskite.

Inclusion MaTroc has a complex history. The POI core probably formed by reaction of an unknown precursor(s) of condensation origin with a vapor to form olivine, plagioclase, clinopyroxene, apatite, and (an) unknown phase(s) that vanished, leaving abundant void space. The spinel-rich mantle is also a secondary mineral assemblage that formed by breakdown of and solid–vapor reactions with a precursor or precursors, possibly melilite (or hibonite). The abundant magnetite formed by reaction of perovskite with an oxidizing vapor and by precipitation from such a vapor. All phases of the inclusion experienced the metasomatic addition of Fe, Ni, and moderately volatile elements such as V, Be, Li, Cr, and Mn—similar to all other constituents of the Maralinga CK chondrite. Phases in MaTroc and in the host rock are close to equilibrium in the distribution of Fe, Mg, Ni, and Mn but far from equilibrium in the distribution of M^{+3} and M^{+4} ions. The minor and trace element abundances in the magnetite of the host rock and of MaTroc preclude an origin by oxidation of a metal precursor.

1. INTRODUCTION

Karoonda (CK) group chondrites are anhydrous and highly oxidized carbonaceous rocks consisting mainly of olivine (Fa28.8–Fa33.3), magnetite and plagioclase (An14–An83) (Kallemeyn et al., 1991). They have refractory lithophile element abundances intermediate between those of CO and CV chondrites and have refractory siderophile element abundances similar to those of CR, CM, and CO chondrites. Maralinga differs from the mainstream CK chondrites in being depleted in Ni, Co, Au, Se, Zn, Mo, and Re (Kallemeyn et al., 1991; Geiger and Spettel, 1991; Kurat et al., 1991), features which Maralinga shares partly with LEW86258. These particular abundance patterns have been interpreted as being probably due to leaching during weathering (both meteorites are finds) (Kallemeyn et al., 1991). However, Kurat et al. (1991) showed, by comparing the Maralinga data with those obtained from experimentally heated Allende samples, that these features are likely to be the result of nebular processing under oxidizing conditions and that Maralinga possibly never received its full share of these elements, which are volatile under oxidizing conditions.

Calcium–aluminum-rich inclusions (CAIs) are rare in CK chondrites. Only one inclusion from Karoonda has been described. This contains the unusual mineral assemblage fassaite–hercynite–olivine (MacPherson and Delaney, 1985). Maralinga seems to contain more CAIs than the average CK chondrite. However, these CAIs are all of unusual mineralogical composition, consisting mainly of hercynite, plagioclase, apatite, and Ca-rich pyroxene. Keller (1992) distinguished four types, which differ from each other in the abundances of the above-mentioned minerals and in their structures/textures. Here we describe a fifth type, similar to the plagioclase–olivine(–pyroxene) inclusions (POIs) previously described from the Lancé (CO), Allende (CV), and other chondrites (Kurat and Kracher, 1980; Wark, 1987; Boctor et al., 1988; Sheng et al.,1991; Jones and Hutcheon, 1996; Russell et al., 1996). This inclusion, which we named Maralinga Troctolite or MaTroc, is unusual

* Author to whom correspondence should be addressed (gero.kurat@univie.ac.at).

because of its size and its complex solar nebula history. A preliminary report was given by Zinner et al. (1995).

2. ANALYTICAL METHODS

The inclusion MaTroc was found on a cut surface of a sample of Maralinga purchased for the collection of the Naturhistorisches Museum in Vienna. A polished thin section (inventory number M8320) was studied with the optical microscope and with an analytical scanning electron microscope (SEM; JEOL SM6400). Mineral analyses were made with an ARL-SEMQ electron microprobe operated at 15 kV and ~10 nA sample current. Measurements were calibrated against mineral standards and corrections were applied following the procedure of Bence and Albee (1968). Attempts at identifying the carrier of refractory elements were made by high-resolution elemental mapping for Ti, Y, Zr, Nb, and Ta with the SEM and a Voyager 2000 system, unfortunately without success.

Trace element and isotope analyses were made in situ with the Cameca IMS 3F ion microprobe at Washington University, St. Louis. Trace element analyses followed a modified procedure of Zinner and Crozaz (1986). Relative ion yields for silicates are those given by Fahey et al. (1987) and for the other phases those given by Ireland et al. (1991). Magnesium isotope measurements were made according to the procedures of McKeegan et al. (1985) and Fahey et al. (1987) and Ti isotope measurements according to those of Fahey et al. (1987) and Ireland (1990).

3. RESULTS

3.1. Petrography

The MaTroc inclusion has a triangular cross section (5 × 2.5 mm) and a zonal structure. It consists of a core, mantle, and crust (Fig. 1). The core is located off center, is round with a diameter of ~1 mm, and has a protrusion extending for an additional 1.5 mm. It consists of a plagioclase–olivine–Ca-rich pyroxene intergrowth with subordinate apatite which form a complex meta-gabbro-like texture (Fig. 2). Large intergranular pore space is partly filled by host matrix olivine and Ca-carbonate. Accessory ilmenite and magnetite are mostly intimately intergrown with or enclosed by the major phases. Some magnetite spherules of ~1μm diameter as well as some small nepheline grains are present in pores. All major minerals contain abundant inclusions of one another and of accessory phases and have variable amounts of empty pores and cracks. Particularly olivine is in places very rich in inclusions of Ca-rich pyroxene and contains traces of very small magnetite (with and without ilmenite) and plagioclase. Subinclusions have complex shapes that locally develop graphic intergrowths. Ca-rich pyroxene is poor in inclusions but has empty voids or voids partly filled by Ca carbonate or nepheline. Plagioclase has commonly inclusions of olivine and Ca-rich pyroxene and is rich in voids of irregular shape. The large voids contain olivine and feathery and porous Ca carbonate. Apatite is coarse-grained (Fig. 2) and commonly has inclusions of plagioclase and Ca-rich pyroxene. Intergrowth of the major minerals is mostly compact, but abundant large intergranular pore space is present in other places (Fig. 3). This pore space is in most cases partially filled by platy and spinoidal olivine (~5–20 μm), fibrous and porous Ca-carbonate (Figs. 3 and 4), and occasionally some nepheline and magnetite spherules. Grain boundaries are usually highly complex without recognizable crystallographic control, except for Ca-rich pyroxene, which develops crystal faces in places, particularly in contact with plagioclase and plagioclase lining intergranular pores (Fig. 4). Textural relationships between

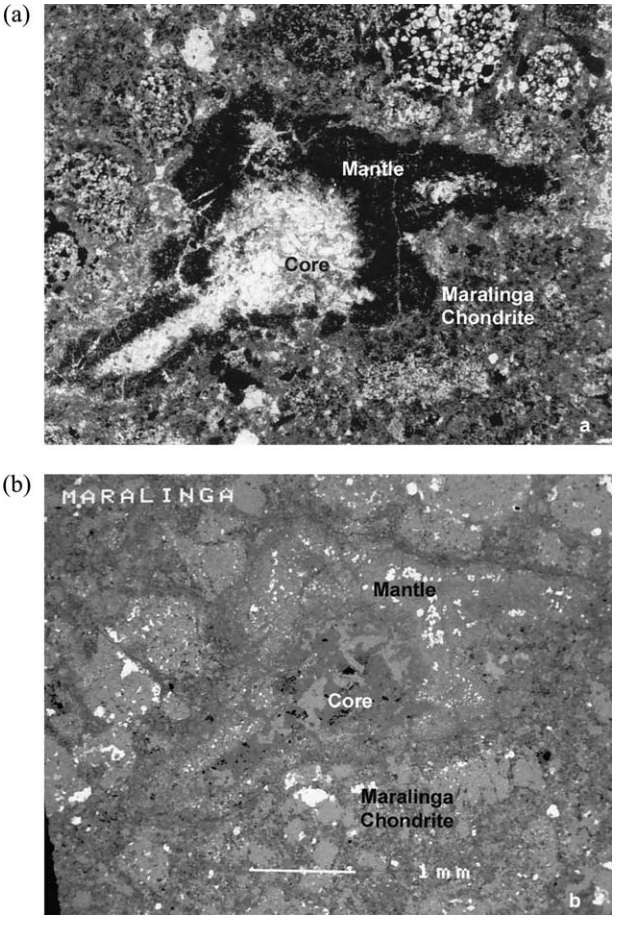

Fig. 1. Overview of the inclusion MaTroc. Note the zonal structure consisting of a coarse-grained troctolitic core (with a peninsular extension, bright in transmitted light), a hercynite–plagioclase–magnetite mantle (black in transmitted light), and a thin crust (barely visible). (a) transmitted light image; (b) back scattered electron (BSE) image.

phases and between phases and pore space are complex in places (Figs. 4 and 5). Pores usually have highly irregular shapes and are commonly lined by Ca-rich pyroxene or complex pyroxene–magnetite intergrowths (Fig. 5).

The mantle of MaTroc is of variable thickness (0.1–1.5 mm) and consists of a compact intergrowth of green spinel (hercynite) and plagioclase with abundant dispersed magnetite grains of widely varying sizes (1–100 μm) and shapes (Figs. 1, 3, and 6). It is highly heterogeneous in the relative abundance of phases and the spinel–plagioclase intergrowths have a sinter or, in places, symplectitic texture and variable plagioclase/hercynite ratios and grain sizes (Figs. 7–9). Matrix plagioclase is usually compact but can be porous in some places. It is poor in inclusions. Plagioclase enveloped by hercynite is very rich in inclusions, which comprise Ca-rich pyroxene, olivine, hercynite, magnetite, and rare sulfides. Hercynite is intimately intergrown with plagioclase and includes abundant plagioclase and occasional magnetite plates. It is very poor in pores. Magnetite (Figs. 6 and 7) has highly irregular grain boundaries and is most abundant in mantle portions rich in hercynite. It is compact and has only few inclusions but contains broad (5 to 10 μm) ilmenite and thin (<1 μm) hercynite lamellae (Fig. 7).

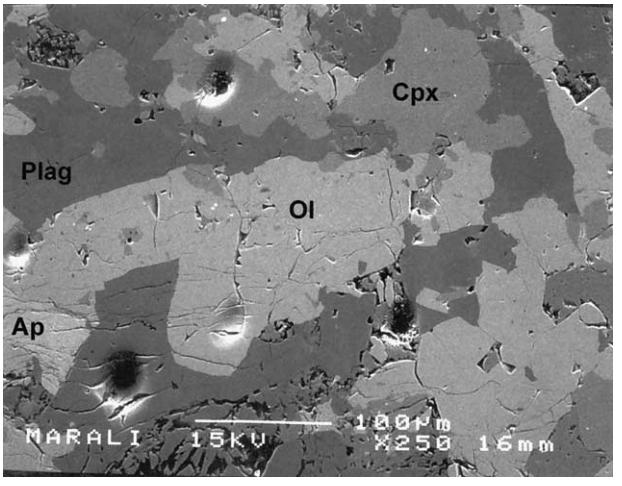

Fig. 2. Detail of MaTroc inclusion core with sputter pits from ion microprobe analysis. The image shows plagioclase–olivine–clinopyroxene intergrowths. Note the complex grain boundaries and the abundant nonspherical inclusions in all phases as well as the abundant pores within coarse grains and the porous matrix in between grains. Ca-pyroxene (Cpx) is gray, plagioclase (Plag) is dark gray, olivine (Ol) is light gray, and apatite (Ap) light-light gray (near lower left corner). Round holes are ablation pits from the ion probe. BSE image.

Near the core–mantle boundary of MaTroc some Ca-rich pyroxene is also present and forms, together with hercynite and plagioclase, concentrically zoned, vermicular intergrowths that commonly contain a central void which is lined by pyroxene. In many places the mantle is cut by plagioclase-rich veins connecting the core with the crust or different regions of the crust (Fig. 6). Minor phases in the mantle are Ca carbonate and olivine in pore space. Very rare are tiny sulfide inclusions (1–2 μm) in plagioclase.

The thin (~5–50 μm) discontinuous crust of MaTroc consists mainly of plagioclase with some olivine and magnetite and

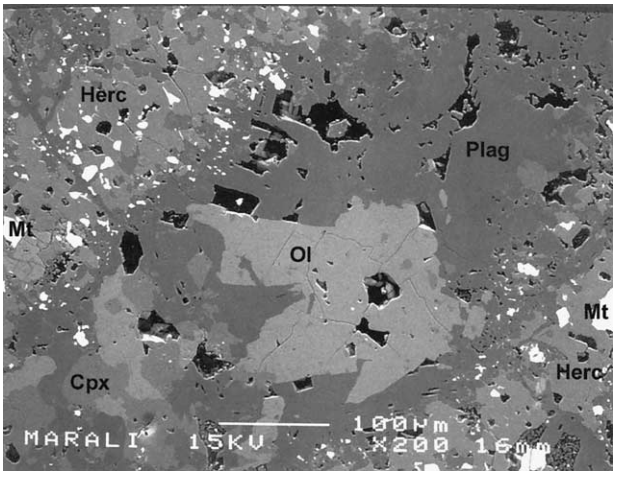

Fig. 3. Detail of MaTroc core lobe from Fig. 1 enveloped by mantle consisting of hercynite (Herc), plagioclase (Plag), and magnetite (Mt). Note the dense and complex intergrowth of olivine (Ol, light gray), plagioclase (dark gray), and Ca-rich pyroxene (Cpx, gray), the distribution and abundance of voids in the core and in the mantle, and the inhomogeneous distribution of the major phases. BSE image.

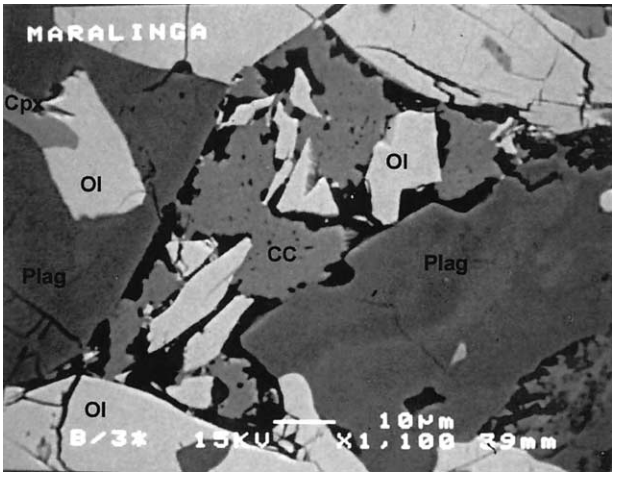

Fig. 4. Detail from Fig. 2; intergranular pore space partially filled by olivine (Ol, light gray) and porous carbonate (CC, gray). Dark phase is plagioclase (Plag—of inhomogeneous composition) with crystal faces developed against the cavity and the olivine (Ol) on the upper left. BSE image.

is in places intimately intergrown with the chondrite matrix. An indentation contains an olivine–plagioclase intergrowth with a micro-gabbro-like texture in places. The surface plagioclase is porous and contains inclusions of hercynite, olivine, and very small (<1 μm) magnetite. Occasionally this crustal plagioclase is intergrown with olivine from the chondrite matrix. A very thin discontinuous skin of either olivine or Ca carbonate covers parts of the inclusion (barely visible in Fig. 9).

The host chondrite Maralinga has been classified as a metamorphosed carbonaceous chondrite of the Karoonda type (CK4; Geiger and Spettel, 1991; Kallemeyn et al., 1991; Kurat et al., 1991; Keller et al., 1992). It has a pronounced chondritic texture with abundant coarse-grained recrystallized aggregates and chondrules and a highly porous matrix (Fig. 1). Maralinga consists mainly of olivine, plagioclase, magnetite, and iron

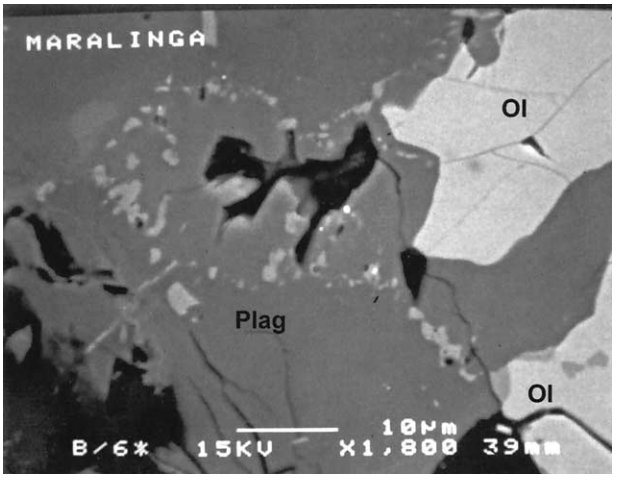

Fig. 5. Detail from MaTroc inclusion core. The open pore space in plagioclase (Plag, center) is decorated by Ca-rich pyroxene which forms a string of tiny grains which extends into olivine (Ol, at lower right). BSE image.

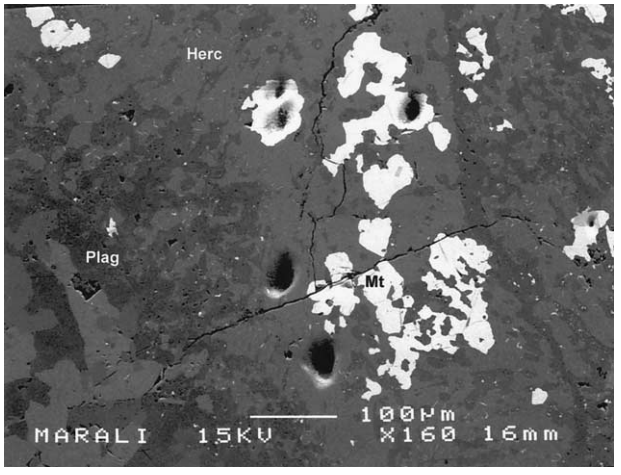

Fig. 6. The MaTroc mantle, detail from Fig. 1. Hercynite (Herc, gray), magnetite (Mt, white), and plagioclase (Plag, dark gray). The contact to the core is to the left and consists of symplectitic intergrowths of hercynite and plagioclase with dispersed magnetite of highly irregular shape. On top of the dense hercynite–magnetite mantle portion is a plagioclase vein followed by a symplectitic hercynite–plagioclase intergrowth with dispersed small magnetites (right margin). Round holes are from the ion microprobe. BSE image.

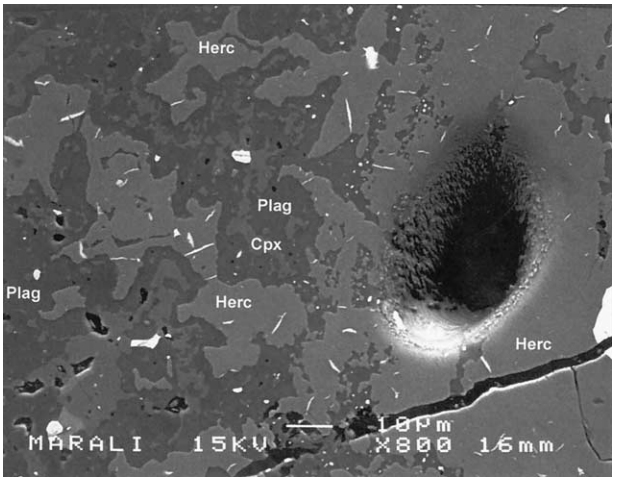

Fig. 8. Detail of the situation in the vicinity of Herc-2 analysis spot (round hole). To the left is a symplectitic intergrowth of hercynite (Herc, gray), plagioclase (Plag, dark gray), and Ca-rich pyroxene (Cpx, gray, in plagioclase). Note the magnetite spindles in hercynite. Some of the bright phases in plagioclase are sulfides. BSE image.

oxide/hydroxide with minor amounts of Ca-rich pyroxene, Ca-poor pyroxene, Ca carbonate, and sulfides (mainly pyrrhotite and pentlandite). Olivine is coarse-grained in aggregates and chondrules (100–300 μm) and contains in some places abundant inclusions of magnetite, plagioclase, and occasionally Ca-rich pyroxene as well as small pores, but in other places it is poor in inclusions and pores. Matrix olivine is granular and forms large and highly porous patches of intimate intergrowths with plagioclase but occasionally is also platy and spinoidal with abundant intergranular pore space. These intergranular pores commonly contain Ca carbonate. Large magnetites are present in aggregates as well as in the matrix. They have complex lobate outlines and contain abundant inclusions of apatite, olivine, plagioclase, and rare pyroxene. A variety of Fe, Ni sulfides is also enclosed by the magnetite, including pentlandite, millerite, and nickeloan pyrite. Magnetites have abundant lamellae of hercynite (two generations, Fig. 10) and two types of ilmenite lamellae. One is broad (1–10 μm) and long ($\sim$<200 μm) and the other is very fine (Fig. 10).

3.2. Mineral Composition: Major Elements

Averaged and selected major and minor elemental compositions of the oxide minerals of Maralinga inclusion MaTroc and

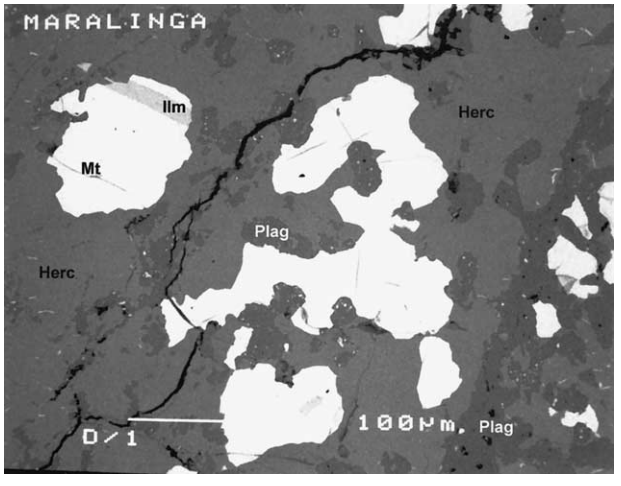

Fig. 7. Detail from Fig. 6 depicting the preanalysis situation. Magnetite (Mt, white) with broad ilmenite (Ilm) lamellae and thin hercynite spindles is intergrown with hercynite (Herc, gray) and plagioclase (Plag, dark gray). Note the symplectite-like texture, the abundant inclusions in plagioclase (mainly magnetite and hercynite, some Ca-rich pyroxene), and the tiny magnetite spindles in hercynite. BSE image.

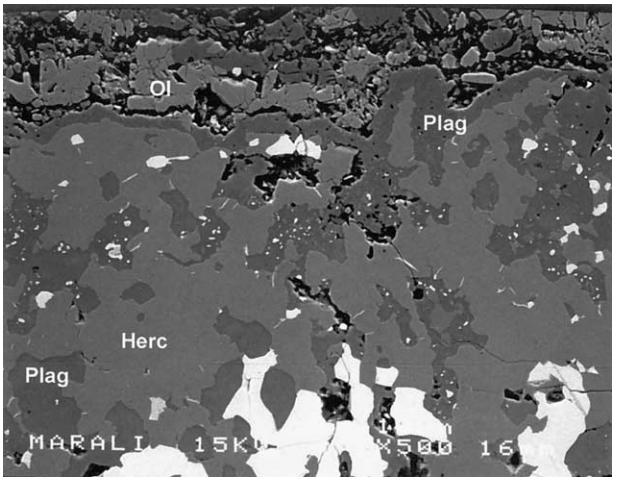

Fig. 9. Detail of the thin crust between the MaTroc inclusion's mantle (lower part) and the chondrite matrix (at upper margin). Here the crust consists of a thin (<10 μm) layer of plagioclase (Plag) which is porous and contains a few tiny olivines (Ol). This plagioclase usually is separated from matrix olivine but occasionally seems to be intergrown with small matrix olivine grains. The very surface is formed by a very thin (<1 μm) olivine supercrust; Herc = hercynite. BSE image.

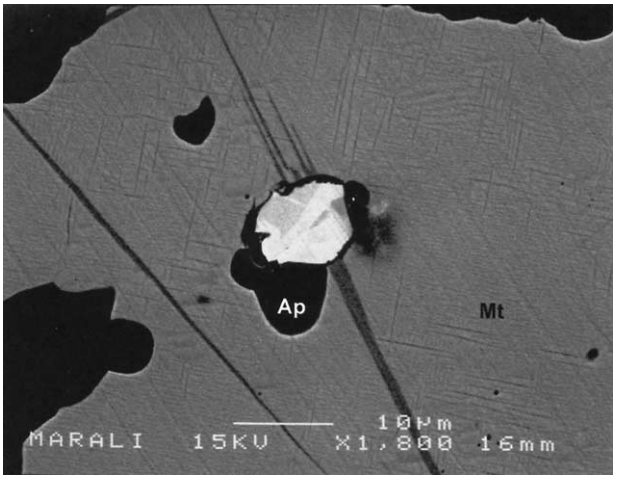

Fig. 10. Detail of Maralinga chondrite magnetite (Mt) with a complex inclusion consisting of apatite (Ap, black) and four different sulfides (gray to white). Thick spindles are hercynite as are the thin oriented spindles. BSE image.

the host chondrite are given in Table 1. The composition of olivines is essentially constant throughout Maralinga with a small range in Fa content from 32 to 34 (average 33.2) mol.%. The minor element contents are usually low (TiO_2, Cr_2O_3, $Al_2O_3 \leq 0.05$ wt.%) in olivines in the inclusion and in the chondrite, except for MnO (~0.23 wt.%), NiO (0.5–0.7 wt.%), and CaO, which has a low abundance in most olivines (<0.05 wt.%) but in olivines of the inclusion (Ol-2 in Table 1) reaches values of ~0.1 wt.%. Clinopyroxene in the inclusion is rich in CaO (23.5 wt.%) and poor in TiO_2 (0.11 wt.%) and Cr_2O_3 (0.05 wt.%), in contrast to the chondrite clinopyroxene, which has less CaO (22.0 wt.%) and more TiO_2 (0.45 wt.%) and Cr_2O_3 (0.55 wt.%). The contents of Al_2O_3, FeO, MnO, MgO, NiO, and Na_2O are similar in clinopyroxene inside and outside the inclusion. Orthopyroxene is only present in the host chondrite, has a composition of En70.6Fs28.6Wo0.8, and has appreciable contents of Al_2O_3, MnO, NiO, and CaO (Table 1; see also Keller et al., 1992). Plagioclase has a compositional range from An55 to An74 with the high-An compositions occurring in the MaTroc inclusion's mantle. The range in the chondritic host is wider, from An20 to An80 (Keller et al., 1992; Keller, 1992). Minor element contents are low. Some FeO is always present (0.3–0.6 wt.%) and the K_2O content increases with decreasing An content from 0.14 to 0.57 wt.%. Magnetites have varying compositions depending on their location. The large magnetites of the MaTroc inclusion's mantle (Mt1 in Table 1) have higher contents of TiO_2, Al_2O_3, MgO, and NiO than the small ones. All of them are poor in Al_2O_3 and Cr_2O_3 compared to magnetites in the host, which however have less NiO than those in the inclusion. Ilmenite from the MaTroc inclusion differs from the host ilmenite in being poor in Cr_2O_3, but both have appreciable MgO and MnO contents. Hercynite associated with the large magnetites in the central mantle of the inclusion (Herc1 in Table 1) differs from hercynite associated with small magnetites in the outer mantle by having much less Cr_2O_3 (0.05 vs. 0.27 wt.%) and somewhat less ZnO (0.45 vs. 0.64 wt.%), but

Table 1. Electron microprobe analyses of major minerals in Maralinga MaTroc inclusion and host chondrite (in wt%).

MaTroc Inclusion

	O11	O12	Cpx	Plag1	Plag2	Plag3	Mt1(L) *	Mt2(S) *	Ilm **	Herc1 ***	Herc2 ****	Ap *****
N	5	4	14	2	3	2	3	2	2	4	10	2
SiO_2	35.1	35.7	53.4	46.7	49.3	52.4	0.03	0.06	0.04	0.06	0.09	
TiO_2	0.03	0.03	0.11				0.64	0.29	53.8	0.05	0.04	
Al_2O_3		0.05	2.06	33.1	31.3	29.1	0.72	0.41	0.04	61.3	60.7	
Cr_2O_3			0.05				0.08	0.18		0.05	0.27	
FeO	30.1	30.1	6.4	0.31	0.33	0.3	89.5	89.2	44.6	26.2	26	0.29
MnO	0.24	0.23	0.08					0.02	0.67	0.09	0.09	
MgO	34.8	33.5	15.7	0.02			0.15	0.06	2.08	12.4	11.9	0.03
NiO	0.63	0.66	0.13				0.72	0.34	0.16	1.53	1.19	
CaO		0.14	23.5	15.2	14	11.4		0.27	0.05	0.03	0.1	53.6
K_2O				0.14	0.18	0.29						
Na_2O			0.33	2.9	3.4	4.9						0.35
Total	100.9	100.41	101.76	98.37	98.51	98.39	91.84	90.83	101.44	101.71	100.38	

*: V_2O_3 = 0.14 wt% **: V_2O_3 = 0.17 wt% ***: ZnO = 0.45 wt% ****: ZnO = 0.64 wt% *****: P_2O_5 = 41.9, C1 = 4.5 wt%.

Maralinga Chondrite

	Mt	Ol	Opx	Cpx	Ilm	Plag
N	7	3	3	5	3	2
SiO_2	0.07	36.5	53.5	52.6	0.06	57.5
TiO_2	0.35		0.02	0.45	52	
Al_2O_3	2.3	0.02	0.5	1.95		25.0
Cr_2O_3	5.7	0.03	0.03	0.55	0.4	
FeO	83.5	29.1	17.7	7	44.9	0.6
MnO	0.05	0.21	0.25	0.09	0.57	
MgO	0.3	34.2	27.1	15.5	1.49	0.03
NiO	0.32	0.52	0.24	0.08	0.05	
CaO		0.02	0.36	22		8.3
K_2O						0.57
Na_2O				0.36		7.0
Total	92.59	100.6	99.7	100.58	99.47	99.0

Ol: olivine; Cpx: Ca-rich pyroxene; Plag: plagioclase; Mt: magnetite; Ilm: ilmenite; Herc: hercynite; Ap: apatite; Opx: low-Ca pyroxene.

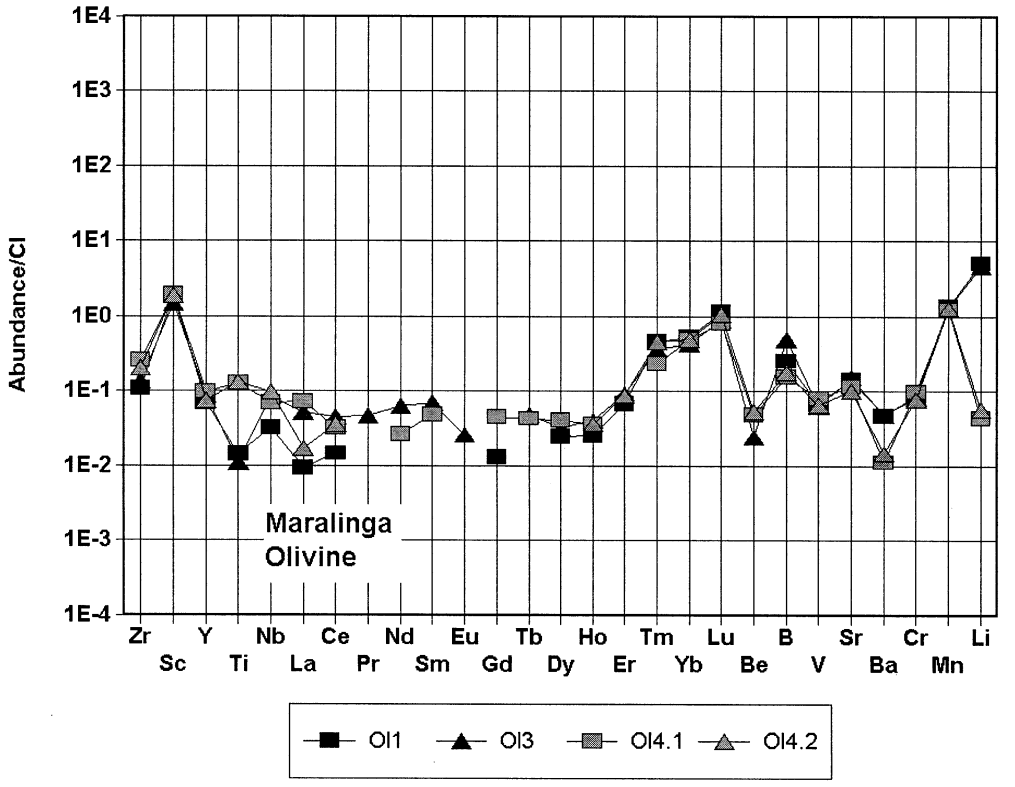

Fig. 11. Trace element abundances in olivines (Ol) from the Maralinga MaTroc inclusion and the host CK4 chondrite. The abundances in this and in subsequent plots are normalized to the CI abundances given by Anders and Grevesse (1989). Elements in all trace element plots are arranged in order of increasing volatility, except for the REE, which are arranged in order of increasing atomic number. Note the similarity in HREE abundances and discrepancy in Li abundances in olivines from the inclusion (black symbols) and from the host chondrite (gray symbols).

being richer in NiO (1.53 vs. 1.19 wt.%). Calcium carbonate (not in the Appendix) contains minor amounts of FeO (0.25 wt.%), NiO (0.03), MgO (0.6), K_2O (0.03), Na_2O (0.03), Al_2O_3 (0.08), and SiO_2 (0.1–0.3 wt.%).

3.3. Mineral Composition: Trace Elements

Abundances of up to 37 trace elements for all major phases of the MaTroc inclusion and of olivine and magnetite from the host chondrite are given in the Appendix.

Most phases are rich in trace elements and have CAI Group II rare earth element (REE) patterns (Martin and Mason, 1974; Mason and Martin, 1977; Wark, 1987), with depletions of the refractory heavy REE (HREE) with respect to the light REE (LREE), a pronounced positive Tm anomaly and, commonly, a negative Eu anomaly. The exceptions are olivine, which has LREE depletions relative to the HREE, and calcite, which does not show any significant REE fractionation at the 1 × CI abundance level.

Olivines (Fig. 11) are typically rich (>1 × CI) in Sc, Lu, Mn, and Li (MaTroc olivines only), have intermediate contents (~0.1 to 1 × CI) of Zr, Tm, Yb, B, Sr, and Ti (host chondrite olivines only), and are poor (<0.1 × CI) in Al, most REE, Y, Ca, Nb, V, Ba, Cr, Be, Ti (MaTroc olivines) and Li (host olivines). Olivines in the MaTroc inclusion have different contents of Ti, Ba, Li and B than those in the host chondrite.

Clinopyroxenes of the MaTroc inclusion have variable and high contents of trace elements, with Sc and most REE at abundance levels >10 × CI (Fig. 12) and Zr, Y, Ti, Eu, Lu, Nb, Be, and B at 1 to 10 × CI abundances. They are poor (<1× CI) in V, Sr, Ba, Cr, Mn, and Li.

Plagioclase in the inclusion's core (Fig. 13) has a steeply fractionated REE pattern with La > Lu (~20 and 0.1 × CI, respectively) and small positive anomalies of Eu and Tm. Most trace element abundances are low (<0.1 × CI), except for Sr (~20 × CI), Ba and Be (~9 × CI). Plagioclase in the inclusion's mantle is 3 to 10 times richer in REE than that in the core, has also a steep REE pattern with La > Lu (~60 and 1× CI, respectively) but has a strong positive Tm anomaly and a weak negative Eu anomaly. Contents of Zr, Y, Ti, Nb, V, Mg, Cr, and Li are higher in mantle than in core plagioclase.

Mantle hercynite (Fig. 14) is rich in trace elements and has a steeply fractionated REE pattern with La > Lu (~15 and 0.7× CI, respectively), a strong negative Eu (Eu/Eu* ~ 0.1) anomaly, and a strong positive Tm (Tm/Tm* ~ 10) anomaly. Here Eu* and Tm* are the Eu and Tm abundances obtained by geometrical interpolation between the neighboring REE of these two elements. Remarkable are the high contents of Zr (2 to 5 × CI), V (~4 × CI), Sr, Ba, and Be (~1 × CI) and the

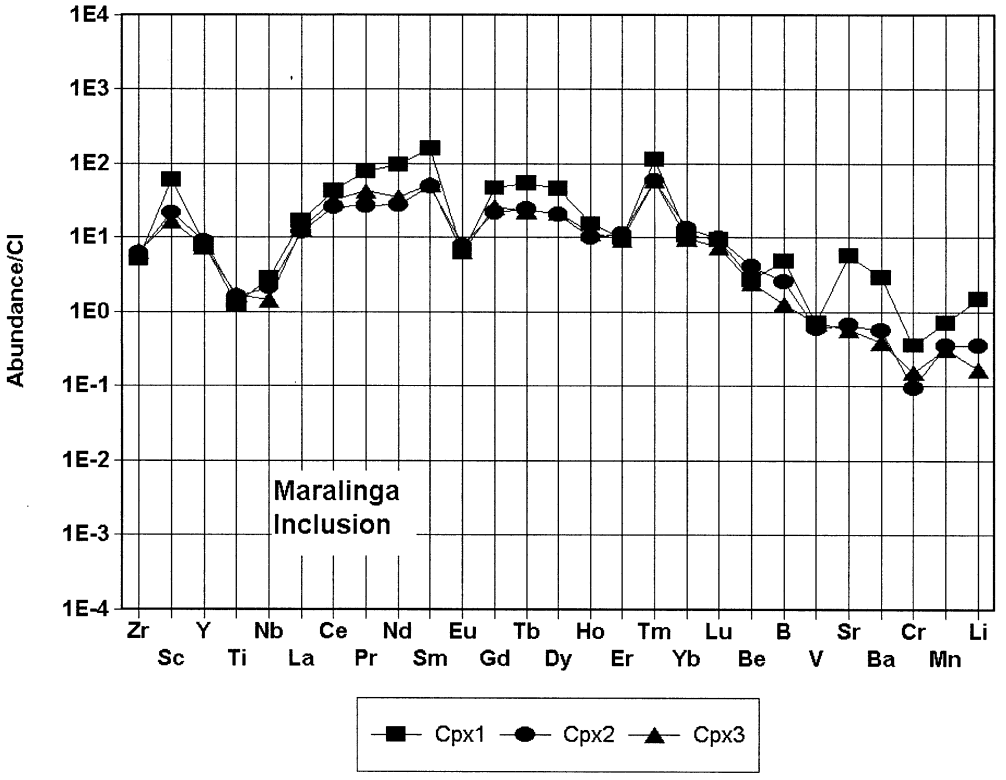

Fig. 12. CI-normalized trace element abundances in Ca-rich pyroxene (Cpx) from the Maralinga MaTroc inclusion. The REE pattern is a CAI group II pattern. Variability of trace element abundances could be due to admixture of "obscurite".

low content of Cr (~0.2 × CI). Large concerted variability is present among the contents of Ti, Nb, Sr, Ba, and Li.

Magnetites show highly heterogeneous trace element patterns (Fig. 15). Inclusion MaTroc magnetite Mt-1 is apparently contaminated by an inferred compound with extremely high trace element concentrations but of unknown nature, which, lacking a better name, we termed "obscurite" (see below). Mt-2 is the trace element–poorest magnetite grain encountered in the inclusion. It is, however, still fairly rich in trace elements, with Zr, Sc, LREE, Tm, Nb, and V being above CI abundances. Its Cr content is very low (~0.1 × CI) as are its contents of Mn, Li, Be, and B. The REE show a steep, fractionated pattern with La > Lu (~12 and 0.5 × CI, respectively) and a strong positive Tm anomaly. Magnetite in the host chondrite is also heterogeneous, with highly variable contents of Zr, Y, Ti, REE, Sr, Ba, and Li. The REE patterns are slightly fractionated with La > Lu (~10 to 2 × CI and 0.5 to 0.1 × CI, respectively). Differences in abundances of more than a factor of 2 exist for REE, Zr, Sr, Ba, and Li. Pronounced differences exist between magnetite inside and outside the MaTroc inclusion in the abundances of Ti, Cr, and Mn, which are low, and LREE, Tm, and Ba, which are high in inclusion magnetite.

"Obscurite" is an unidentified compositional relic, present mainly in magnetite, possibly also in Ca-rich pyroxene, which carries large amounts of refractory trace elements (Fig. 16). It is very rich in REE, which have a CAI group II abundance pattern, and in Y, Be, B, and V and rich in Zr, Sc, Ti, Sr, and Ba. Despite the very high trace element counts, we were unable to make this phase visible. Despite our inability to identify obscurite, for simplicity we shall use this term for the rest of this paper.

Apatite (Fig. 17) is rich in Y, REE, Sr, and Ba with the REE abundances gently declining from LREE abundances of ~100× CI to Lu at ~25 × CI and displaying small anomalies for Eu(−) and Tm(+). The elements Zr, Sc, Nb, Li, and Be have also superchondritic abundances (all at ~2–4 × CI).

Calcium carbonate (Fig. 17) has low and unfractionated REE contents (~0.5 × CI), low Li and Be contents (~0.01 × CI), and is rich in Sr and Ba (>10 × CI).

An ilmenite lamella (Fig. 17) intergrown with magnetite is rich in Nb (~800 × CI), V (~50 × CI), Sc (~20 × CI), and Hf and Zr (~10 × CI). The REE abundances range from ~3× CI (La) to 0.4 × CI (Er) with Y (~0.1 × CI) indicating that HREE abundances might be even lower and with Tm being overabundant (~3 × CI) with respect to Er.

3.4. Isotopes

A search for ^{26}Al in plagioclase was mostly negative, with only one measurement giving a small ^{26}Mg excess. The Ti isotope ratios in ilmenite are normal, as expected.

4. DISCUSSION

4.1. Shape, Structure, and Textures

The shape of inclusion MaTroc (Fig. 1) is clearly nonfragmental, and the lobate outline and the smooth botryoidal sur-

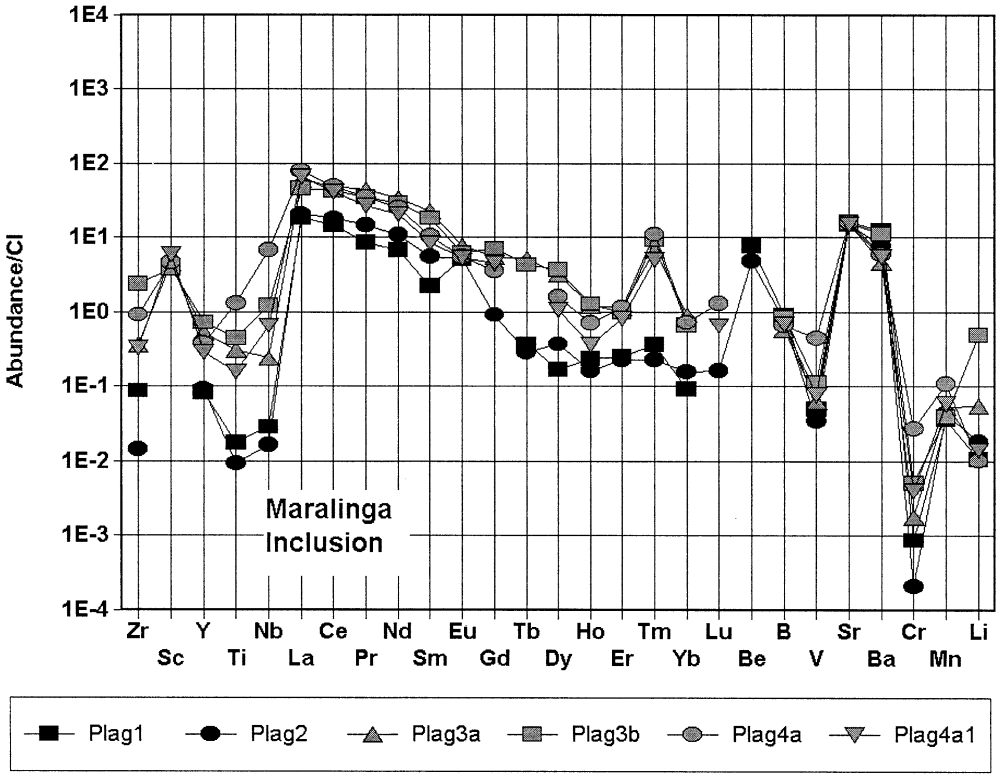

Fig. 13. CI-normalized trace element abundances in plagioclase (Plag) from the Maralinga MaTroc inclusion. Core plagioclase (black symbols) are poorer in trace elements than mantle plagioclase (gray symbols), except for Sr and Ba. The REE patterns are fractionated CAI group II patterns which is well preserved in the mantle plagioclase but almost obliterated in core plagioclase.

face are reminiscent of terrestrial mineral precipitation from diluted solutions. The triangular shape of the cross section indicates a tetrahedral shape in three dimensions, a shape possibly indicative of diffusion-controlled growth, as is also indicated by the lobes that evidence growth along preferential directions. The overall structure of MaTroc—core, mantle, and crust—suggests sequential formation under changing conditions with incomplete adaptation (reaction) to the continuously created new conditions.

The MaTroc inclusion is covered by Maralinga chondrite matrix–like material, the troughs more so than the hills. Nowhere is the inclusion directly in contact with any larger constituents of Maralinga (chondrules, aggregates, fragments, etc.). This must be taken as evidence for the accretion of matrix material onto MaTroc and the other constituents before incorporation into the Maralinga rock. As there are some small-scale intergrowths of the MaTroc crust with matrix olivine, the inclusion has possibly already existed when Maralinga matrix olivines formed.

The texture of MaTroc's POI core, when viewed superficially, feigns an igneous origin. Indeed, POIs like the core of MaTroc are widely believed to be of igneous origin (Sheng et al., 1991). A closer look (Figs. 2 and 3), however, reveals that it must have had a more complicated and certainly nonigneous genesis. Grain boundaries are highly complex and out of equilibrium. All major phases carry abundant inclusions of one another and also of minor phases, which have highly irregular (nonequilibrated) shapes. One major constituent of MaTroc's POI core is void space. Voids are usually ignored but we believe that they should be taken into consideration when discussing the genesis of a rock. The voids in MaTroc's core are not only abundant (Figs. 1 and 3) but they are big—their size is comparable to that of the other constituents—and they have irregular shapes similar to those of the other constituents. Their morphology strongly suggests that they formerly contained a mineral(s) that became unstable during processing of MaTroc and broke down into mobile species which subsequently vanished. The abundant small voids likely are of a similar origin. Some of the large voids are partly filled with olivine that is morphologically similar to olivine in the Maralinga chondrite matrix and with obviously late deposited Ca carbonate (Figs. 2–4). The very complex relationship between all phases and the voids suggests formation via breakdown and solid–fluid reactions of precursor phases.

The symplectitic texture of MaTroc's mantle is extremely complex with highly unequilibrated grain boundaries and grain size distribution. A solid–fluid reaction at subsolidus temperature and of short duration (with no grain boundary equilibration) appears to be the most likely mechanism for the creation of such a texture.

4.2. Mineral Assemblage and Chemistry

Mineral assemblages change dramatically from MaTroc core to mantle and vary also within the mantle. The assemblage

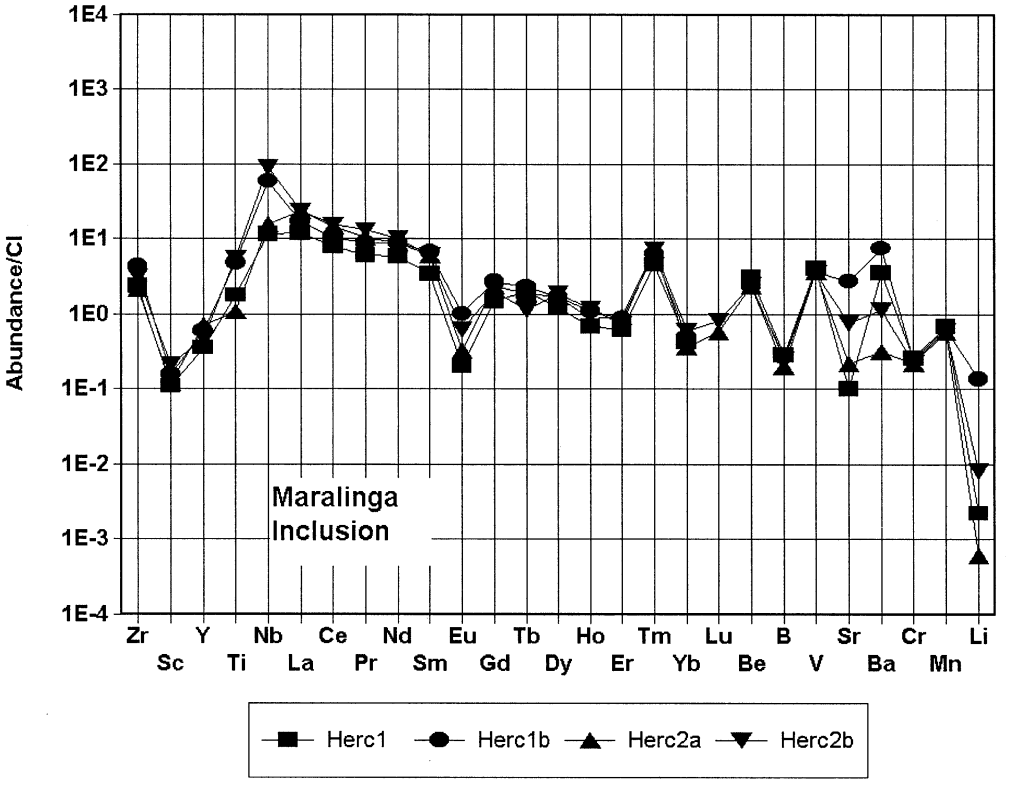

Fig. 14. CI-normalized trace element abundances in hercynite (Herc) from the mantle of the Maralinga MaTroc inclusion. Trace element abundances are fairly homogeneous. Variability in Ti, Eu, Sr, Ba, and Li abundances is likely due to plagioclase and ilmenite inclusions.

within the core consists of (in order of abundance): plagioclase, olivine, clinopyroxene, and apatite. Such a mineral association could represent an (unusual) igneous rock, a P-rich gabbroic troctolite with micro-gabbro texture. Phase abundances vary from place to place (Fig. 1) as does the abundance of omnipresent angular voids. The presence of abundant apatite is not compatible with the cosmochemically refractory bulk composition of MaTroc's core. Obviously, P must originally have been carried by a refractory phase. As only reduced P phases (e.g., schreibersite, barringerite) behave as cosmochemically refractory phases, the large amount of P present in MaTroc's core could point towards a reduced refractory precursor mineral assemblage.

The mantle is dramatically different in texture and mineral assemblage: it consists of hercynite, plagioclase, magnetite, and voids with minor clinopyroxene (Fig. 1). The mineral association obviously is that of a CAI; the magnetite, however, seems to be out of place as CAIs normally carry neither large amounts of metal nor Fe-oxides. Keller (1992) reports the presence of magnetite in all four types of CAIs present in Maralinga, but apparently in none of them is magnetite a major phase—in stark contrast to MaTroc which thus represents a fifth type. In any case, this assemblage clearly is of nonigneous origin—as is the texture, as discussed above.

Fe, Mg-mineral have been described to be compositionally homogeneous in Maralinga (Keller et al., 1992). This is also what we find in the Maralinga host rock. However, the phases in inclusion MaTroc have compositions that deviate somewhat from those of the host rock minerals. In particular, clinopyroxene in MaTroc is poorer in TiO_2 and Cr_2O_3 than clinopyroxene in the Maralinga host chondrite (0.11 and 0.05 wt.% vs. 0.45 and 0.55 wt.%, respectively, see Table 1) and richer in CaO (23.5 vs. 22.0 wt.%). Also, magnetite in MaTroc is poorer in Al_2O_3 and Cr_2O_3 than magnetite in the host chondrite ($\sim$0.5 and $\sim$0.15 vs. 2.3 and 5.7 wt.%, respectively). Apparently, Fe, Mg, Ni, and Mn have equilibrated in silicates throughout Maralinga, whereas Ca, Cr, and Ti have not. The high Ca content of the clinopyroxene in MaTroc indicates a lower temperature of equilibration in the inclusion than in the chondrite. The latter has been estimated to be between 650°C (Geiger and Bischoff, 1995) and 750 to 850°C (Noguchi, 1993) which is somewhat lower than that estimated for the Kobe CK chondrite ($\sim$850°C, Tachibana et al., 2001). The low Ti content of the MaTroc clinopyroxene points into the same direction: As the Ti activity in the system is buffered by ilmenite, the low content in clinopyroxene indicates a low temperature of equilibration. The low Cr content seems simply to be a consequence of the very low bulk Cr content of the inclusion MaTroc. Apparently, diffusive homogenization did not work on a mm scale.

Magnetite compositions are also dramatically different in MaTroc and the host chondrite (Appendix). Again, the low contents of Al and Cr in MaTroc magnetites indicate low-temperature distribution of Al between phases and a low bulk Cr content of MaTroc. The high contents of Ti, Al, and Cr in magnetites of the Maralinga host chondrite clearly indicate that the magnetite is not the product of oxidation of former Ni-Fe metal as advocated by

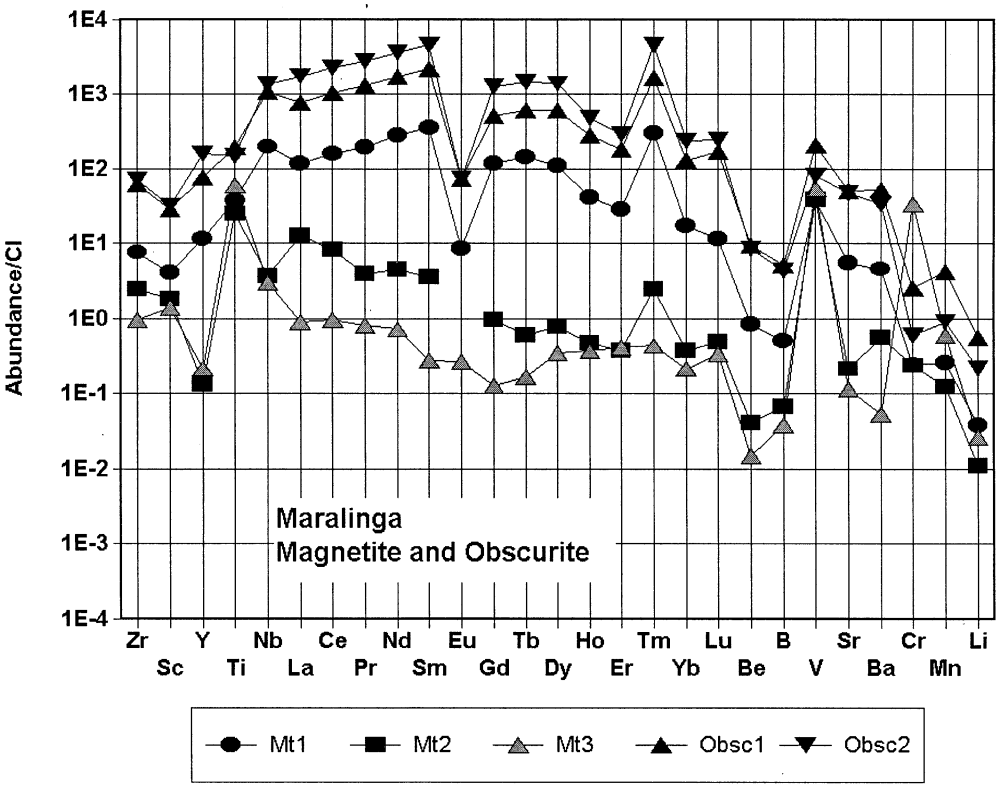

Fig. 15. CI-normalized trace element abundances in magnetite (Mt) from the Maralinga MaTroc inclusion (black symbols) and the host chondrite (gray symbols). Note the differences in the abundances of Ti, LREE, Tm, and Cr in the magnetites from inside and outside the inclusion. MaTroc magnetites have highly variable trace element contents due to admixture of variable amounts of "obscurite" (Obsc) which has a slightly modified group II CAI trace element pattern.

Geiger and Bischoff (1995) because in that case the magnetite should not contain any lithophile elements (Kurat et al., 1991).

4.3. Trace Element Distribution

All phases of inclusion MaTroc that are large enough to be analyzed with the ion probe are rich in trace elements (Appendix, Figs. 11–17). Trace element abundances in all phases have patterns similar to that of group II CAIs (Ireland and Fegley, 2000). This pattern is common among CAIs from CV and CM chondrites and very common among CAIs from CH chondrites (Weber and Bischoff, 1994; Weber et al., 1995). Because the group II CAI trace element pattern is depleted in the cosmochemically most refractory (e.g., Lu, Zr, Y, Ho) and in the relatively volatile (Ba, Nb, Yb, Eu, Si) elements with respect to intermediate refractory ones (e.g., Tm, Nd, Sm, La, Ce), it is evidence for a genesis via condensation from a vapor which was depleted in the most refractory elements (Boynton, 1975). Consequently, inclusion MaTroc or at least some of its precursors must have a condensation origin.

4.4. MaTroc Core

4.4.1. Olivine

Olivine is the only phase with a trace element pattern that does not show any obvious relationship to those of the other phases (Figs. 11 and 17). The exception is a small positive Tm anomaly, mimicking the Tm excesses in the other phases of MaTroc's core. Otherwise, the pattern seems to roughly follow the olivine-melt distribution coefficients.

Closer inspection reveals that a hypothetical melt in equilibrium with olivine (distribution coefficients from Green, 1994) would be very rich in the LREE (La $\sim$ 300 $\times$ CI), Sr, Ba, and in Nb ($\sim$650 $\times$ CI) and also rich in the HREE (Lu $\sim$ 30 $\times$ CI), Y, Zr, and Sc. However, the Ti content of the hypothetical melt could have been only at the chondritic level, in accordance with the overall group II CAI elemental abundance pattern of MaTroc and the low Cr and V abundances. Surprising is the high Li content of the MaTroc olivine which is almost 100 times as high as that of the common Maralinga olivines. The Mn content is in agreement with partitioning from a chondritic source (as is the Fe content). Because these elements were very likely added to the system late in the history of MaTroc (and of all other constituents of Maralinga), one needs a source of only chondritic composition for the metasomatic exchange reaction between Fe-free original olivine and the vapor (compare Kurat, 1988). The high Li content could indicate that MaTroc olivine was present when Li became oversaturated in the vapor. Apparently, olivine of the MaTroc inclusion records an attempt to equilibrate with a system very rich in trace elements and with an abundance pattern similar to that of group II CAIs.

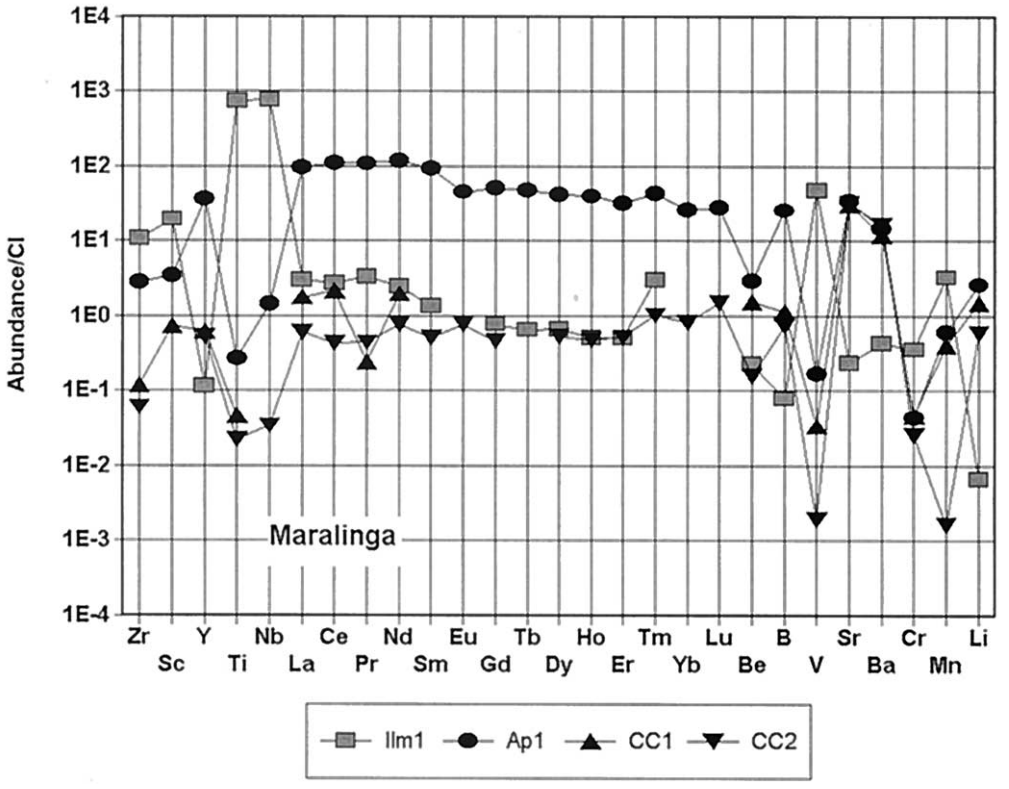

Fig. 16. CI-normalized trace element abundances in apatite (Ap) and Ca-carbonate (CC) from the Maralinga MaTroc inclusion core (black symbols) and in ilmenite (Ilm) from the inclusion's mantle (gray symbol). Apatite and ilmenite have modified group II CAI REE pattern, that of the Ca carbonate is unfractionated at about chondritic abundance.

4.4.2. Clinopyroxene

Clinopyroxene of the MaTroc core has high trace element contents (up to >100 × CI) and a typical group II CAI pattern (Figs. 12 and 17). Trace element abundances are variable (up to a factor of 10—see Sr). The group II CAI pattern is only slightly modified [the CI-normalized ratio (Sm/La)n = 4–10] according to the clinopyroxene– liquid distribution coefficients (Green, 1994). A hypothetical liquid in equilibrium with clinopyroxene is very rich in LREE (La ~ 380 × CI), Nb (~200 × CI), and Ba (~380 × CI), rich in Zr (~70 × CI), Y (~20 × CI), Sc (10 × CI), and Sr (~10 × CI), and poor in Ti, V, and Cr. Obviously, this hypothetical liquid also has a group II CAI pattern, but at a considerably higher level than the average group II CAI (Ireland and Fegley, 2000).

Variability of trace element contents in clinopyroxene suggests admixture of trace elements carried by a separate phase. The concerted increase of, e.g., Tm, Sm, Sr, Ba, and Sc makes it likely that the admixed phase is "obscurite," an unknown trace element carrier present in large amounts in the magnetite of MaTroc's mantle (see below). That carrier could either be dissolved in clinopyroxene or distributed as solid grains. Because the LREE abundances in clinopyroxene attempt to follow the $K_D^{cpx\text{-}liqu.}$ it is very likely that the REE are dissolved in the clinopyroxene. In any case, the carrier probably was a solid that was added to the growing clinopyroxene in variable amounts, resulting in trace element heterogeneity.

4.4.3. Plagioclase

Plagioclase in the MaTroc core is trace element– rich but less so than in the mantle (Figs. 13 and 18). The REE abundances in the core plagioclase show a normalized pattern that is subparallel to the plagioclase–liquid distribution coefficient. This means that the REE elements are dissolved in the plagioclase structure. Europium shows only a small positive abundance anomaly mirroring an Eu-poor (relative to the other REE) environment. A hypothetical liquid in equilibrium with MaTroc core plagioclase (distribution coefficients from Irving, 1978 and Yurimoto and Sueno, 1984) is very rich in LREE (~200 × CI), rich in HREE (~20 × CI), Be (~10 × CI), Eu (~8 × CI), Sr (~3 × CI), and poor in Ti (~0.3 × CI), V (~1 × CI), and Li (~0.3 × CI). This again is a signature of the group II CAI abundance pattern. Trace elements in the MaTroc core plagioclase appear also to be inhomogeneously distributed, indicating admixture of variable amounts of a trace element carrier. This carrier was subsequently dissolved but not homogenized in the plagioclase.

Apatite of MaTroc core is rich in REE and a few other trace elements. The REE display an almost flat abundance pattern with LREE > HREE and small anomalies for Eu(−) and Tm(+), indicating a relationship to a parent with a group II CAI abundance pattern (Fig. 17). The REE abundance pattern closely follows the apatite–liquid distribution coefficients (Watson and Green, 1981). A hypothetical liquid in equilibrium with apatite is rich in LREE (La ~30 × CI), HREE (Lu ~15

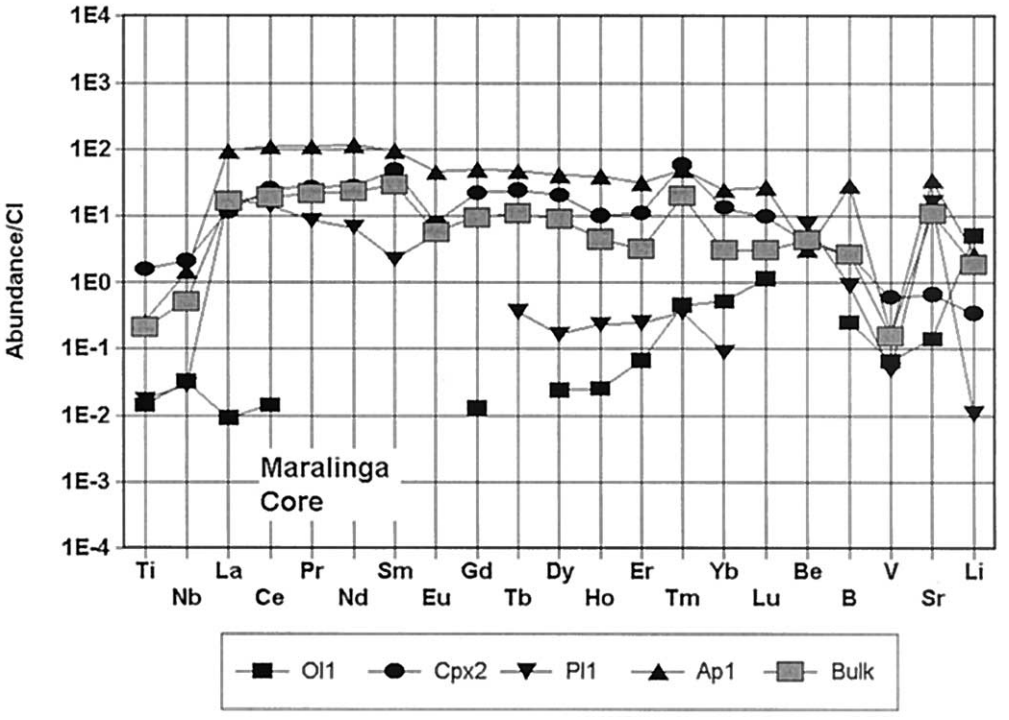

Fig. 17. CI-normalized trace element abundances in primary minerals of the core of the Maralinga MaTroc inclusion. Note that the group II CAI REE pattern is strongly modified in all phases.

$\times$ CI), and Sr ($\sim$15 $\times$ CI). These abundances are very similar to those of the estimated MaTroc core bulk (see below), indicating that apatite almost achieved chemical equilibrium with the bulk core system. This is no surprise because of all the phases present apatite has the highest diffusion rates for REE and other trace elements. Apatite appears to roughly have achieved chemical equilibrium with the bulk core system, despite the fact that all other phases are far from equilibrium with each other and the bulk system.

4.4.5. Calcium carbonate

Calcium carbonate partly fills voids in MaTroc's core (Fig. 4) and obviously has a late origin, very likely independent of the rest of the rock. As Maralinga is a find, the carbonate could have a terrestrial source. However, the REE abundances are approximately chondritic (Fig. 16) and thus make a terrestrial origin unlikely. Some other elements (Li, Mn, B, Be, Y, Sc) are also present at about chondritic abundance levels, others (Sr, Ba, V, Ti, Nb, Zr) follow the carbonate/silicate distribution coefficients. Because equilibrium seems not to have been achieved, a low-temperature transient event appears to be responsible for the formation of the carbonate. It could have precipitated from a CO_2-rich fluid with trace elements buffered by a chondritic source.

4.4.6. Bulk MaTroc core

Using rough estimates of the major phase abundances in the MaTroc core (plagioclase—50, olivine—30, clinopyroxene—15, apatite—5 wt.%) we can calculate its bulk trace element contents (Fig. 17). They are very similar to those of the average group II CAI pattern as calculated by Ireland and Fegley (2000). However, the MaTroc abundance pattern differs from the average group II CAI pattern by being much smoother, being less depleted in HREE, more strongly depleted in Ti, V, and Nb, and not depleted in Sr. Surprisingly high are the Li, Be, and B contents, for which, however, no data exist for comparison and which definitely deserve a separate study.

4.4.7. Summary MaTroc core

The MaTroc core is a POI with a micro-gabbro-like texture and group II CAI trace element abundances. Unlike other POIs, which are considered to be igneous rocks (Sheng et al., 1991), MaTroc clearly has a nonigneous origin as is demonstrated by the abundance of voids, the highly complex, nonequilibrated grain boundaries, the nonequilibrated grain sizes, and the nonequilibrium trace element contents of its major phases.

MaTroc's core has average group II CAI trace element abundances and, consequently, it or its precursors must have a condensation origin from a vapor depleted in the superrefractory trace elements. The trace elements now reside in the rock-forming minerals but possibly were introduced into the system residing in refractory dust that was inhomogeneously distributed among and within the phases. MaTroc core POI, as it is now, has not seen very high temperatures and has not experienced melting and therefore grossly preserved trace element heterogeneity. This is also supported by the Mg isotope heterogeneity observed by Sheng et al. (1990) in POIs from the Allende, Leoville, and Adelaide chondrites.

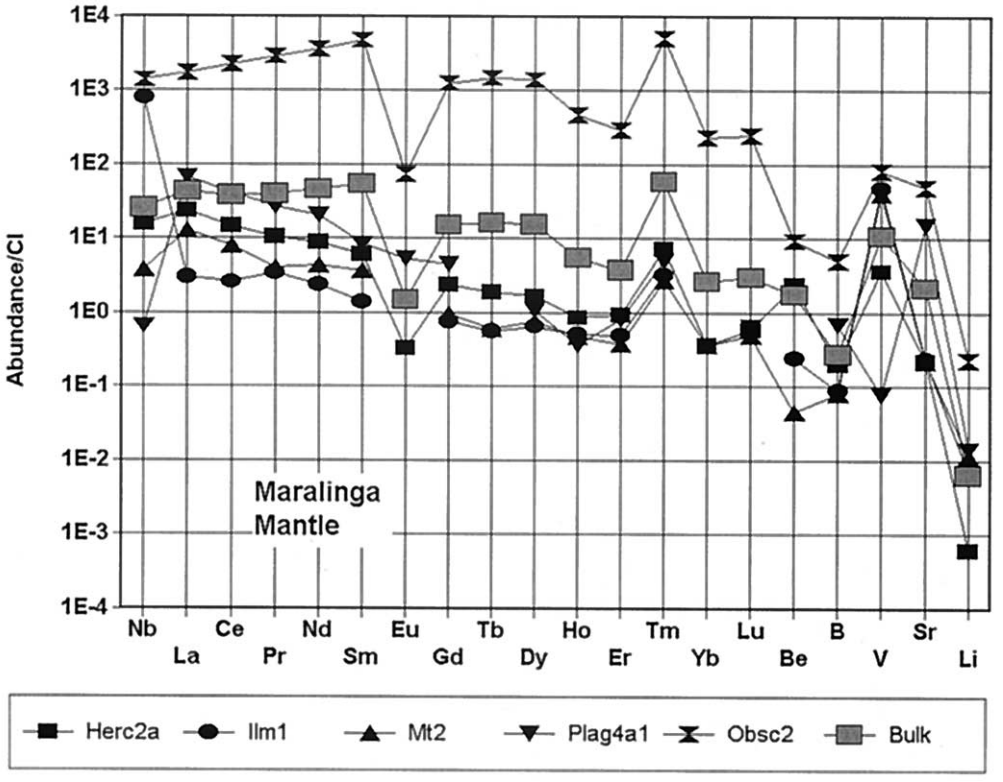

Fig. 18. CI-normalized trace element abundances in minerals of the mantle of the Maralinga MaTroc inclusion. The group II CAI REE pattern appears to be modified in all phases.

4.5. MaTroc Mantle

4.5.1. Plagioclase

Plagioclase of MaTroc mantle is very rich in trace elements, much richer than the plagioclase of MaTroc core (Figs. 13 and 18). The REE abundance pattern shows a steep decrease from La to Ho [CI-normalized ratio (La/Ho)n ~ 100] and a strong positive Tm anomaly. In addition, the abundances of high field strength elements (HFSE) are 10 to 100 times higher in MaTroc mantle plagioclase than in that from the core. Most trace elements have variable abundances, indicating derivation from inhomogeneously distributed precursor(s) and lack of equilibration. A hypothetical melt in equilibrium with plagioclase (distribution coefficients from Irving, 1978 and Yurimoto and Sueno, 1984) is very rich in Sc, the LREE and Tm (>400 × CI), rich in HREE (~100 × CI), Be and Ti (~10 × CI), Eu (~8 × CI), and Sr (~2 × CI) and poor in V, Cr, and Li. These abundances closely match those of group II CAIs, albeit at a very high level.

Because plagioclase has either no or only a small negative Eu anomaly, the structural preference for Eu^{2+} obviously could not overcome the low Eu abundance of the whole system. This fact indicates that the REE (and possibly all other trace elements) are dissolved in the plagioclase lattice. The strong positive Tm anomaly thus reflects the high abundance of this element in the system. Because the REE pattern parallels that of the plagioclase– liquid partition coefficients, there was an attempt to approach equilibrium of the trace element abundances. The variable contents of trace elements in different plagioclase grains, however, indicate that equilibrium was not achieved and that the precursors themselves had nonequilibrium trace element contents. Because these inhomogeneities persist at the 10 to 20 μm scale, temperatures must have been low during processing of MaTroc—in accordance with observations in MaTroc's core. The very high REE abundances appear to be the result of high abundances in the precursor phase and of the fact that of all major phases present, plagioclase is the phase with the highest acceptance for REE.

4.5.2. Hercynite

This is the most abundant phase in MaTroc's mantle and it is very rich in trace elements (Figs. 14 and 18). The REE display a pattern with a steep slope from La (~15 × CI) to Yb (~0.4 × CI) and with anomalies of Eu(−) and Tm(+). This pattern does not agree with the spinel/liquid distribution coefficient pattern (Nagasawa et al., 1980) which displays a slope in the opposite direction. The hypothetical liquid in equilibrium with MaTroc hercynite is very rich in LREE (~10,000 × CI) and HREE (~30 × CI), rich in Zr (~10 × CI), and poor in V (~0.2 × CI) and Cr (~0.005 × CI). These abundances are highly unusual and do not make very much sense. We are forced to assume that hercynite carries the trace element pattern of a precursor(s).

Because the trace element pattern of hercynite in many features is similar to that of the coexisting anorthite and be-

cause hercynite occurs in a texturally highly unequilibrated symplectitic intergrowth with anorthite, both phases could have the same precursor. One possible and likely precursor phase is melilite, which could have reacted with the vapor to form spinel and anorthite. If we assume that hercynite retained the trace element pattern of its precursor melilite, we can calculate the composition of a liquid in equilibrium with such a melilite (melilite– liquid partition coefficients from Green, 1994). This liquid is rich in LREE (~30 × CI) and HREE (~2 × CI), is very rich in Tm (~50 × CI), in Zr (~2000 × CI), and is poor in Eu and Sr (~1 × CI) and Be (~2 × CI). These abundances match those of the average group II CAIs (Ireland and Fegley, 2000), except for Zr (and possibly also Ti and Nb), and those in melilite of inclusion ALH3 from the Allende chondrite (Simon et al., 2001). We argue that this good match supports a derivation of hercynite (and anorthite) from a melilite precursor, a view which is supported by the symplectitic intergrowth of these two breakdown phases. The reaction could have been:

$$\underset{\text{gehlenite}}{2Ca_2Al_2SiO_7} + \underset{\text{vapor}}{MgO} = \underset{\text{spinel}}{MgAl_2O_4} + \underset{\text{anorthite}}{CaAl_2Si_2O_8} + \underset{\text{lime}}{3CaO} \quad (1a)$$

if the reaction took place early, before FeO became a stable species in the vapor, or

$$\underset{\text{gehlenite}}{2Ca_2Al_2SiO_7} + \underset{\text{vapor}}{FeO} = \underset{\text{hercynite}}{FeAl_2O_4} + \underset{\text{anorthite}}{CaAl_2Si_2O_8} + \underset{\text{vapor}}{3CaO} \quad (1b)$$

if it took place under oxidizing conditions which creates a volatile Ca species ($Ca(OH)_2$, Hashimoto, 1992). However, reaction (1a) with deposition of CaO and subsequent mobilization of CaO as $Ca(OH)_2$ could have created the abundant voids present.

Most trace element abundances fit this scenario but Zr and the other HFSEs need a separate carrier. Such a carrier is indicated also by the variable abundances of Nb, Ti, and perhaps Sr and Ba. The trace element abundances in MaTroc hercynite are very similar to those of melilites from grossite-bearing CAIs in Acfer 182 (Weber et al., 1995), except for the positive Yb anomaly displayed by the Acfer 182 melilites. The pattern is also similar to some patterns of spinel-rich CAIs in Mighei (MacPherson and Davis, 1994).

Another possible precursor could have been hibonite which typically has REE contents at 10 to 1000 × CI abundances (Ireland, 1990; Ireland et al., 1988; Simon et al., 2001). Hibonite also accommodates HFSEs much better than melilite. Reaction with the ambient vapor as described by Fahey et al. (1994) from a hibonite–hercynite CAI from Lancé will produce a spinel-rich mineral assemblage. It could also easily produce a spinel–anorthite assemblage.

4.5.3. Magnetite and obscurite

MaTroc's magnetite is—as are all other phases—also surprisingly rich in trace elements (Figs. 15 and 18) and it has extremely variable trace element contents. Obviously, we see mixing of at least two components: magnetite and a phase extremely rich in trace elements, obscurite. Magnetite with the lowest trace element contents encountered (Mt-2) has an abundance pattern similar to that of hercynite, just at a somewhat lower level. The REE pattern has a slope from La to Yb, with a CI-normalized ratio $(La/Yb)_N$ of ~35, and it has a pronounced positive Tm anomaly. A hypothetical liquid in equilibrium with Mt-2 (distribution coefficients from Nielsen et al., 1992, Nielsen 1994, and Nielsen and Beard, 2000) is very rich in LREE (La ~ 2500 × CI) and HREE (Lu ~ 50 × CI), Zr (~100 × CI), and Ti (~35 × CI), and poor in Sc (2 × CI), Mn and Cr (<0.1 × CI). Clearly, the pattern is not that of magnetite (which should have the opposite slope in the REE abundances) but rather that of another phase. It is a modified group II CAI trace element pattern with a Nb/Ti fractionation opposite to that found in the coexisting obscurite. Thus, the magnetite with the lowest trace element content of MaTroc mantle likely contains a trace element carrier that differs from obscurite in being poor in Nb. Another possibility is that at an earlier stage magnetite did dissolve some obscurite at high temperature and kept most of the trace elements but partitioned Nb (and some Ti) into ilmenite exsolutions.

Magnetite with trace element patterns at higher than the lowest level all carry the signature of the unknown phase obscurite with an abundance pattern that is a pure group II CAI pattern at a superrefractory level (Ireland and Fegley, 2000). This pattern is surprisingly similar to that of perovskite in inclusion ALH3 (Simon et al., 2001) and to that of ilmenite in inclusion Axtell Porky (Caillet and Zinner, 1995). Obscurite, therefore, could simply be the trace element signature of the precursor perovskite from which magnetite formed. Conversion of perovskite into ilmenite (and armalcolite) by reaction with Fe^{2+} from the vapor (see below) is very common in CM chondrites and micrometeorites (MacPherson and Davis, 1994; Kurat et al., 1994). Apparently, the reaction went beyond the usual final product in CM chondrites, ilmenite, leading to precipitation of magnetite which dissolved the Ti as ulvöspinel. Thereby the magnetite inherited the trace elements from the original perovskite. Their abundances seem to be grossly unaltered in those portions of magnetite that represent the original perovskite. A slight increase in the abundances of the LREE from La to Sm is typical for Ca-rich group II CAIs, as are the relatively high abundances of Er and Lu. The obscurite carries, in addition to REE, also Zr, Sc, Y, Nb, Be, B, Sr, and Ba, but not much Ti and V. Attempts to locate and identify this phase with SEM and secondary ion mass spectrometry (SIMS) failed—it appears to be dissolved in the magnetite or very finely disseminated and the nanoSIMS (and transmission electron microscopy) will hopefully give an answer. In any case, magnetite of MaTroc mantle not only is an abundant phase but is also a major carrier of lithophile trace elements, a feature not previously observed.

The very high abundances of lithophile trace elements in magnetite, even if they reside in a separate carrier phase, preclude an origin of the magnetite by oxidation of a precursor metal. Oxidation of such large amounts of metal should also produce platinum group elements (PGE) nuggets, which have not been found. Magnetite of MaTroc mantle likely is a secondary phase derived from a nonmetallic precursor, very likely perovskite.

4.5.4. Ilmenite

Ilmenite appears to be a secondary phase, the product of oxidation and exsolution from the magnetite. Its trace element pattern (Figs. 16 and 18) closely follows that of the host magnetite, except for Nb, which is strongly partitioned into the ilmenite. A hypothetical liquid in equilibrium with ilmenite (distribution co-

efficients from Nielsen et al., 1992) is very rich in LREE and Nb (La ~ 400 × CI), HREE (Lu ~ 25 × CI), Zr (~20 × CI), and poor in V (4 × CI), Sr (~2 × CI), and Cr (<0.1 × CI). As ilmenite also displays a positive Tm anomaly, this pattern is very similar to the group II CAI abundance pattern.

4.5.5. Bulk MaTroc mantle

Calculated from rough estimates of the major phase abundances in the MaTroc mantle (hercynite—70, magnetite—19, plagioclase—10, obscurite—1 wt.%), the bulk trace element abundances (Fig. 18) follow a typical group II CAI abundance pattern. Compared to that of MaTroc's core (Fig. 17), the mantle is richer in trace elements and has a trace element pattern that has much more similarity with the average group II CAI pattern (Ireland and Fegley, 2000) than that of MaTroc's core. Interestingly, the core has deficits in Nb and V and surpluses of Li, Be, B, and Sr. These differences are likely related to the different precursors of core and mantle and to the different susceptibility of the phases now present to solid–gas exchange reactions.

4.5.6. Summary MaTroc mantle

The MaTroc mantle differs fundamentally from MaTroc's core and can be classified as a magnetite–spinel CAI, a CAI type only known from Maralinga. It has a classical group II CAI trace element abundance pattern and, consequently, it or its precursor(s) must be the product of condensation from a vapor which was depleted in the most refractory lithophile elements. Spinel–plagioclase symplectite forms the main mass of the mantle and apparently formed by breakdown of preexisting melilite (or hibonite). Magnetite carries an invisible phase, obscurite, which is extremely rich in trace elements with a group II CAI abundance pattern similar to that of perovskite in the ALH3 CAI from the Allende chondrite (Simon et al., 2001). Magnetite by no means can be the product of oxidation of precursor metal. Its very high trace element content as well as the presence of obscurite make it likely that magnetite is a reaction and oxidation product of a highly refractory precursor, possibly perovskite.

4.6. MaTroc's Complex Sequential History

Reconstruction of the sequential history of MaTroc is possible but must remain fragmentary. From evidence outlined above we can construct the following sequence of events which ultimately produced MaTroc:

The first condensates formed from a vapor already depleted in the most refractory elements. The conditions were reducing and phosphide(s) were among the first mineral assemblage which formed an aggregate that later will become the core. On top of this aggregate, melilite (or hibonite) plus perovskite were deposited which also condensed from a vapor already depleted in the most refractory elements. As redox conditions in the vapor changed (presumably because of cooling), the reduced mineral assemblage of the core was oxidized. The mineral assemblage changed, maybe in cascades, ending up as a plagioclase–olivine–clinopyroxene–apatite rock. Calcium, Al, Ti, and P were likely present from the beginning; the other elements must have been acquired from the vapor. As we do not know the original mineral assemblage, we can not reconstruct solid–vapor interactions in detail.

The mantle melilite of MaTroc reacted with the vapor as indicated in Eqns. (1a) and (1b). Both reactions possibly took place and ultimately formed hercynite and anorthite. The small amount of clinopyroxene present in the mantle could easily also be created by adding more Si to the assemblage. Very likely, there was also a reaction of Fe^{2+} from the vapor with perovskite:

$$2CaTiO_3 + FeO = Fe^{2+}Ti_2O_5 + 2CaO$$

perovskite vapor armalcolite vapor (2)

Subsequently, armalcolite could have reacted to form ilmenite

$$Fe^{2+}Ti_2O_5 + FeO = 2Fe^{2+}TiO_3$$

armalcolite vapor ilmenite (3)

which further reacted to ulvöspinel:

$$Fe^{2+}TiO_3 + FeO = TiFe_2O_4$$

ilmenite vapor ulvöspinel (4)

During that stage also Na and K were partly exchanged for Ca in anorthite (Kurat and Kracher, 1980) modifying it to plagioclase ~An60–An74. Olivine and clinopyroxene of the core exchanged Fe, Mn, and Cr for Mg (Kurat, 1988). As oxygen fugacity continued to increase Fe^{3+} became available, and magnetite formed and dissolved the ulvöspinel to form titanomagnetite. Magnetite continued to precipitate until the abundant accessible pore space was used up. As a result MaTroc mantle became very rich in magnetite and this magnetite had variable amounts of ulvöspinel dissolved. Because the trace elements, which originally were present in large amounts in perovskite, stayed mostly immobile, parts of the magnetite that mark the original location of the perovskite are very rich in trace elements, they contain obscurite. During this stage, Ni^{2+} became available and was exchanged for Mg with silicates and oxides. Upon further cooling some of the ulvöspinel dissolved in magnetite exsolved in an oxidation reaction forming ilmenite exsolution lamellae. Very late in the history of MaTroc, Ca carbonate precipitated into some voids that were accessible to the vapor.

4.7. Maralinga Chondrite

For comparison, a few grains of the major minerals of the Maralinga chondrite were also analyzed with the ion probe (Appendix, Figs. 11 , 15, and 19). Olivines are surprisingly rich in trace elements—comparable to olivine from MaTroc's core (Fig. 11). The LREE and Nb display a flat CI– normalized abundance pattern and the HREE reach CI abundance levels. One grain from the vicinity of MaTroc has a very small positive Tm anomaly, similar to that of the olivines in MaTroc's core. Olivine 4 is located ~0.8 mm from MaTroc's edge in the plane of the section. The presence of a Tm anomaly in this olivine suggests that some elemental exchange took place between MaTroc and Ol-4. That must have happened after Maralinga formed. However, because only one measurement of the two performed on that grain shows the anomaly, it could be a contamination at the grain's surface introduced during polishing.

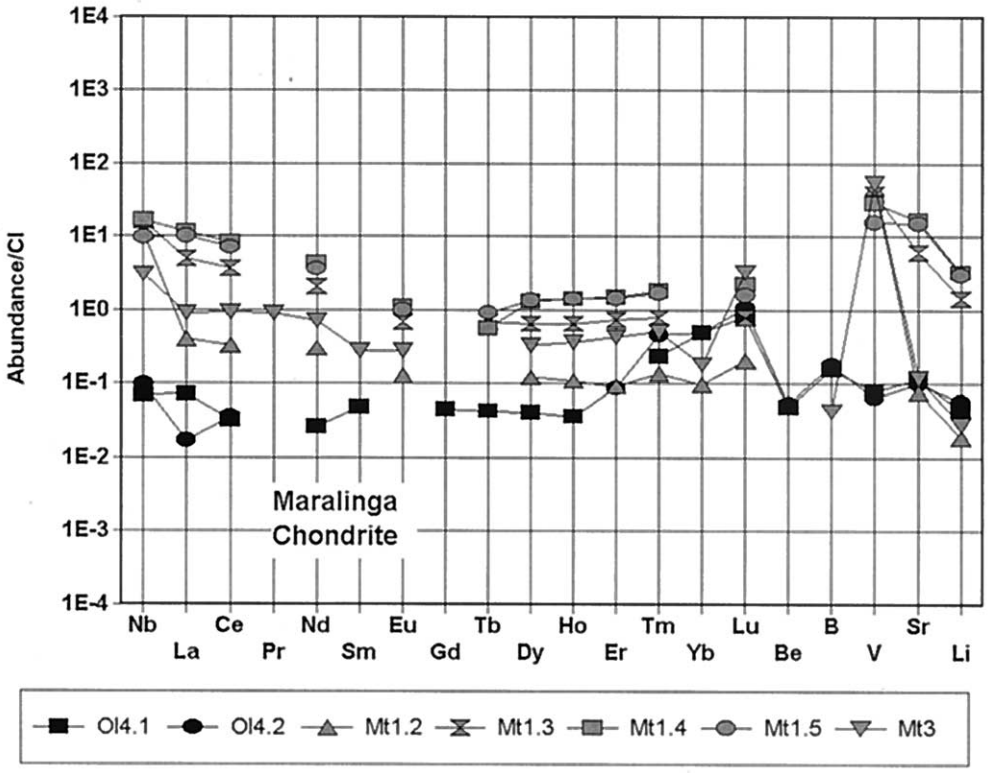

Fig. 19. CI-normalized trace element abundances in olivines (Ol, black symbols) and magnetite (Mt, gray symbols) of the Maralinga host chondrite. Magnetites have high and variable lithophile trace element contents, giving evidence against a derivation from former metal.

Magnetite in the Maralinga chondrite has very high and highly variable contents of lithophile refractory trace elements. The abundance patterns of the REE are slightly fractionated with LREE > HREE, a pattern that is in disagreement with the magnetite–liquid distribution coefficients (Nielsen et al., 1992), which slope into the other direction. The high and variable trace element contents of Maralinga magnetite make it likely that some of them reside in carrier phases. The high Sr and Li abundances found in some grains suggest that one of these carriers could be plagioclase, which is common as inclusion in magnetite. But many other mineral inclusions from Maralinga magnetite have been described (Kurat et al., 1991; Geiger and Bischoff, 1995). However, not all of the variability can be attributed to grains of other minerals because magnetites in Maralinga show highly variable contents of Cr, Al, and Ti. This fact has been used to challenge the belief of Geiger and Bischoff (1995) that Maralinga magnetite formed by oxidation of precursor metal (Kurat et al., 1991). The high and variable trace element contents of the magnetites support the suggestion made (Kurat et al., 1991) that magnetites are precipitates from a vapor. This view is also supported by Hiyagon et al. (2001) who found magnetites of the Kobe CK4 chondrite to have O isotope abundances that are indistinguishable from those of the olivines and which join them by projecting onto the carbonaceous chondrite anhydrous mineral (CCAM) line in the three isotope plot.

5. CONCLUSION

The shape, structure, and texture of MaTroc indicate a complex formation history which involved formation and subsequent breakdown in solid–vapor reactions of unknown and a few identified precursor phases. The mineral assemblage of the core and the nonequilibrium mineral assemblage of the mantle indicate formation at temperatures well below the solidus of the system. Minerals from the host chondrite are out of chemical equilibrium with the minerals of MaTroc. Thus, the constituents must have experienced separate processing before incorporation into the Maralinga rock.

MaTroc's POI core has group II CAI trace element abundances and, consequently, it or its precursors must have a condensation origin. As the trace element abundances show signs of structural control, they must now be dissolved in the phases. Thus, the trace elements now reside in the rock-forming minerals but possibly were introduced into the system by (a) refractory precursor(s). This precursor(s) was transformed into an unknown number of successor phases, finally into olivine, plagioclase, clinopyroxene, and apatite. The trace elements were not mobilized and possibly ended up in a superrefractory dust that was inhomogeneously distributed among and within the final phases. The mineral assemblage of the final core has never seen very high temperatures and has not experienced melting and therefore preserved trace element heterogeneity within and in between phases. Apatite is a common phase of

MaTroc's core, a major carrier of trace elements. It appears to approximately have achieved chemical equilibrium with the bulk core system, even though all other phases are far from equilibrium with each other and the bulk system. The large amounts of P present in the core could indicate a highly reduced refractory mineral assemblage in the original core with P being carried by phosphides.

MaTroc's mantle differs fundamentally from its core and can be classified as a magnetite–spinel-anorthite CAI, a CAI type only known to occur in Maralinga. It has a symplectitic texture and a classical group II CAI trace element abundance pattern. It, consequently, is the breakdown product of a precursor(s) which must be of condensation origin, like the POI core. Spinel is the most common phase and likely formed by breakdown in solid–vapor reactions of preexisting melilite (or hibonite), as did the plagioclase. Magnetite carries an invisible phase, obscurite, which is extremely rich in trace elements with a group II CAI abundance pattern. The presence of obscurite makes it likely that magnetite is a reaction and oxidation product of a highly refractory precursor, possibly perovskite. Magnetite and plagioclase have inhomogeneous trace element distributions which persist at the 10 to 20 μm scale, indicating that temperatures must have been low during processing, in accordance with observations in MaTroc's core. Hercynite carries a trace element record of its precursor, which probably was melilite (or hibonite) that became unstable during nebular processing of the inclusion.

The history of MaTroc has been complex and records changing redox conditions ranging from highly reducing (phosphide stability) to strongly oxidizing (magnetite stability).

Acknowledgments—This work was financially supported by the FWF, Austria and by NASA grant NAG5-9801. Critical and constructive reviews by Trevor Ireland, Michail Nazarov, Ahmed ElGoresy, an anonymous reviewer, and the associated editor Uli Ott have considerably improved this report.

Associate editor: U. Ott

REFERENCES

Anders E. and Grevesse M. (1989) Abundances of the elements: Meteoritic and solar. *Geochim. Cosmochim. Acta* **53,** 197–214.

Bence A. E. and Albee A. L. (1968) Empirical correction factors for the electron microanalysis of silicates and oxides. *J. Geol.* **76,** 382–403.

Boctor N. Z., Hutcheon I. D., and Wasserburg G. J. (1988) (1988) Petrology of a plagioclase-rich forsterite-bearing Allende inclusion abstract. *Lunar Planet. Sci.* **19,** 110–111.

Boynton W. V. (1975) Fractionation in the solar nebula: Condensation of yttrium and the rare earth elements. *Geochim. Cosmochim. Acta* **39,** 569–584.

Caillet C. and Zinner E. (1995) The "Porky" inclusion from the Axtell carbonaceous chondrite: A hercynite-bearing condensate with large calcium-48 and titanium-50 excesses abstract. *Meteoritics* **30,** 494–495.

Fahey A. J., Zinner E. K., Crozaz G., and Kornacki A. S. (1987) Microdistributions of Mg isotopes and REE abundances in a Type A calcium-aluminum-rich inclusion from Efremovka. *Geochim. Cosmochim. Acta* **51,** 3215–3229.

Fahey A. J., Goswami J. N., McKeegan K. D., and Zinner E. (1987) ^{26}Al,^{244}Pu, ^{50}Ti, REE, and trace element abundances in hibonite grains from CM and CV meteorites. *Geochim. Cosmochim. Acta* **51,** 329–350.

Fahey A. J., Zinner E., Kurat G., and Kracher A. (1994) Hibonite-hercynite inclusion HH-1 from the Lancé (CO3) meteorite: The history of an ultrarefractory CAI. *Geochim. Cosmochim. Acta* **58,** 4779–4793.

Geiger T. and Bischoff A. (1995) Formation of opaque minerals in CK chondrites. *Planet. Space. Sci.* **43,** 485–498.

Geiger T. and Spettel B. (1991) Maralinga—A new metamorphosed carbonaceous chondrite abstract. *Lunar Planet. Sci.* **22,** 433–434.

Green T. H. (1994) Experimental studies of trace-element partitioning applicable to igneous petrogenesis—Sedona 16 years later. *Chem. Geol.* **117,** 1–36.

Hashimoto A. (1992) The effect of H_2O gas on volatilities of planet-forming major elements: I. Experimental determination of thermodynamic properties of Ca-, Al-, and Si-hydroxide gas molecules and its application to the solar nebula. *Geochim. Cosmochim. Acta* **56,** 511–532.

Hiyagon H., Nakamura T., and Nakamura N. (2001) An ion microprobe study of oxygen isotopes in the Kobe CK4 meteorite. *Antarct. Meteorites* **26,** 35–37 (abstract).

Ireland T. R. (1990) Presolar isotopic and chemical signatures in hibonite-bearing refractory inclusions from the Murchison carbonaceous chondrite. *Geochim. Cosmochim. Acta* **54,** 3219–3237.

Ireland T. R. and Fegley B. Jr. (2000) . The solar system's earliest chemistry: Systematics of refractory inclusions. *Intl. Geol. Rev.* **42,** 865–894.

Ireland T. R., Fahey A. J., and Zinner E. K. (1988) Trace-element abundances in hibonites from the Murchison carbonaceous chondrite: Constraints on high-temperature processes in the solar nebula. *Geochim. Cosmochim. Acta* **52,** 2841–2854.

Ireland T. R., Fahey A. J., and Zinner E. K. (1991) Hibonite-bearing microspherules: A new type of refractory inclusions with large isotopic anomalies. *Geochim. Cosmochim. Acta* **55,** 367–379.

Irving A. J. (1978) A review of experimental studies of crystal/liquid trace element partitioning. *Geochim. Cosmochim. Acta* **42,** 743–770.

Jones R. H. and Hutcheon I. D. (1996) Mineralogy and secondary alteration of a complex plagioclase-rich inclusion in Kainsaz abstract. *Meteoritics Planet. Sci.* **31,** (Suppl.) A67–A68.

Kallemeyn G. W., Rubin A. E., and Wasson J. T. (1991) The compositional classification of chondrites: V. The Karoonda (CK) group of carbonaceous chondrites. *Geochim. Cosmochim. Acta* **55,** 881–892.

Keller L. P. (1992) Petrography and mineral chemistry of calcium- and aluminum-rich inclusions in the Maralinga CK4 chondrite abstract. *Lunar Planet. Sci.* **23,** 671–672.

Keller L. P. (1993) Heterogeneous plagioclase compositions in the Maralinga CK4 chondrite. Lunar Planet. Sci. XXIV. Lunar Planet. Inst., Houston pp. 783–784.

Keller L. P., Clark J. C., Lewis C. F., and Moore C. B. (1992) Maralinga, a metamorphosed carbonaceous chondrite found in Australia. *Meteoritics* **27,** 87–91.

Kurat G (1988) Primitive meteorites: An attempt towards unification. *Phil. Trans. R. Soc. Lond.* **A325,** 459–482.

Kurat G. and Kracher A. (1980) Basalts in the Lancé carbonaceous chondrite. *Z. Naturforsch.* **35a,** 180–190.

Kurat G., Brandstätter F., Palme H., Spettel B., and Prinz M. (1991) Maralinga (CK4): Record of highly oxidizing nebular conditions abstract. *Meteoritics* **26,** 360.

Kurat G., Hoppe P., and Maurette M. (1994) Preliminary report on spinel-rich CAIs in an Antarctic micrometeorite. Lunar Planet. Sci. XXV. Lunar Planet. Inst., Houston. pp 763–764 (abstract).

MacPherson G. J. and Davis A. M. (1994) Refractory inclusions in the prototypical CM chondrite, Mighei. *Geochim. Cosmochim. Acta* **58,** 5599–5625.

MacPherson G. J. and Delaney J. S. (1985) A fassaite–two olivine-pleonaste-bearing refractory inclusion from Karoonda. Lunar Planet. Sci. XVI. Lunar Planet. Inst., Houston. pp. 515–516 (abstract).

Martin P. M. and Mason B. (1974) Major and trace elements in the Allende meteorite. *Nature* **249,** 333–334.

Mason B. and Martin P. M. (1977) Geochemical differences among components of the Allende meteorite. *Smithson. Contrib. Earth Sci.* **19,** 84–95.

McKeegan K. D., Walker R. M., and Zinner E. K. (1985) Ion microprobe isotopic measurements of individual interplanetary dust particles. *Geochim. Cosmochim. Acta* **49,** 1971–1987.

Nagasawa H., Schreiber H. D., and Morris R. V. (1980) Experimental mineral/liquid partition coefficients of the rare earth elements (REE), Sc and Sr for perovskite, spinel and melilite. *Earth Planet. Sci. Lett.* **46,** 431–437.

Nielsen R. L. and Beard J. S. (2000) Magnetite-melt HFSE partitioning. *Chem. Geol.* **164,** 21–34.

Nielsen R. L., Gallahan W. E., and Newberger F. (1992) Experimentally determined mineral-melt partition coefficients for Sc, Y, and the REE for olivine, orthopyroxene, pigeonite, magnetite and ilmenite. *Contrib. Mineral. Petrol.* **110,** 488–499.

Nielsen R. L., Forsythe L. M., Gallahan W. E., and Fisk M. R. (1994) Major- and trace- element magnetite-melt partitioning. *Chem. Geol.* **117,** 167–191.

Noguchi T. (1993) Petrology and mineralogy of CK chondrites: Implications for the metamorphism of the CK chondrite parent body. *Proc. NIPR Symp. Antarct. Meteorites* **6,** 204–233.

Russell S. S., Huss G. R., Wasserburg G. J., and MacPherson G. J. (1996) Plagioclase-rich inclusions from the Coolidge meteorite: A distinct CAI population with no evidence for radiogenic ^{26}Mg abstract. *Meteoritics Planet. Sci.* **31,** (Suppl) A119–A120.

Sheng Y. J., Hutcheon I. D., and Wasserburg G. J. (1990) Mg isotope heterogeneity in Plagioclase olivine inclusions. Lunar Planet. Sci. XXI. Lunar Planet. Inst., Houston. pp. 1138–1139 (abstract).

Sheng Y. J., Hutcheon I. D., and Wasserburg G. J. (1991) Origin of plagioclase-olivine inclusions in carbonaceous chondrites. *Geochim. Cosmochim. Acta* **55,** 581–599.

Simon S. B., Davis A. M., and Grossman L. (2001). Formation of orange hibonite, as inferred from some Allende inclusions. *Meteoritics Planet. Sci.* **36,** 331–350.

Tachibana Y., Hirajima T., Kitamura M., Nakamura N. (2001) Equilibration temperature of the Kobe meteorite. *Antarct. Meteorites* **26,** NIPR, Tokyo, 133–134 (abstract).

Wark D. A. (1987) Plagioclase-rich inclusions in carbonaceous chondrite meteorites: Liquid condensates? *Geochim. Cosmochim. Acta* **51,** 221–242.

Watson E. B. and Green T. H. (1981) Apatite/liquid partition coefficients for the rare earth elements and strontium. *Earth Planet. Sci. Lett.* **56,** 405–421.

Weber D. and Bischoff A. (1994) The occurrence of grossite ($CaAl_4O_7$) in chondrites. *Geochim. Cosmochim. Acta* **58,** 3855–3877.

Weber D., Zinner E., and Bischoff A. (1995) Trace element abundances and magnesium, calcium, and titanium isotopic compositions of grossite-containing inclusions from the carbonaceous chondrite Acfer 182. *Geochim. Cosmochim. Acta* **59,** 803–823.

Yurimoto H. and Sueno S. (1984) Anion and cation partitioning between olivine, plagioclase phenocrysts and the host magma: A new application of ion microprobe study. *Geochem. J.* **18,** 85–94.

Zinner E. and Crozaz G. (1986) A method for the quantitative measurement of rare earth elements in the ion microprobe. *Int. J. Mass Spectrom. Ion Processes* **69,** 17–38.

Zinner E., Brandstätter F., and Kurat G. (1995) A plagioclase-olivine-spinel-magnetite inclusion from Maralinga (CK): A record of sequential condensation abstract. *Meteoritics* **30,** 605–606.

APPENDIX. Ion microprobe analyses of minerals in Maralinga MaTroc inclusion (I) and host chondrite (Chon; in ppm).

Phase	01-1	01-2	01-3	01-4.1	01-4.2	Cpx-1	Cpx-2	Cpx-3
Locus	I-core	I-core	I-core	Chon	Chon	I-core	I-core	I-core
Element								
Li	7.6	3.8	6.9	0.064	0.085	2.2	0.52	0.25
Be		0.0009	0.0006	0.0012	0.0013	0.067	0.1	0.06
B	0.22	0.29	0.43	0.13	0.16	4.1	2.2	1.1
Na	18.4	4.6	56.2	2.92	1.22	2223	2182	2264
Mg	224400	227200	222700	270800	26900	150300	10000	95700
Al	104	26	287	155	150	8240	13850	15120
Si	163400	163449	163449	163449	247509	247509	247509	
P	270	65	146	2.7	1.8	366	389	111
K	3.4	4.4	10.5	20	15	235	68	60
Ca	106	47	320	66	66	106000	160900	168900
Sc	11	4.8	8.5	11	11	350	125	98
Ti	6.2	3.5	4.7	55.5	56.8	541	692	748
V	3.7	3.2	3.6	4.45	3.6	39	34	40
Cr	224	202	218	258	205	946	251	407
Mn	2660	2520	2570	2390	2500	1410	681	626
Co	1140	1120	1140	1110	1150	519	151	129
Rb	3.1	28	29	5.5	1.8	13	5.4	4.7
Sr	1.11	0.87	1.2	0.89	0.79	45	5.1	4.5
Y	0.11	0.15	0.13	0.15	0.11	12	14	11
Zr	0.42	0.71	0.54	1	0.8	20	24	26
Nb	0.008	0.041	0.021	0.017	0.024	0.69	0.52	0.35
Ba	0.11	0.05	0.11	0.026	0.034	6.9	1.3	0.9
La	0.0022	0.031	0.012	0.017	0.004	3.9	2.8	3.1
Ce	0.009	0.06	.028	0.02	0.022	27	16	20
Pr		0.0073	0.0042			6.9	2.4	3.8
Nd		0.034	0.029	0.012		44	13	16
Sm		0.009	0.01	0.007		23	7	7.4
Eu		0.0015	0.0014			0.35	0.43	0.35
Gd	0.0026	0.005		0.009		9.3	4.4	5.1
Tb		0.0018	0.0017	0.0015		1.9	0.86	0.8
Dy	0.006	0.01	0.008	0.01		11	5	5.3
Ho	0.0014	0.003	0.0022	0.002	0.002	0.85	0.56	0.63
Er	0.011	0.014	0.015		0.014	1.6	1.8	1.5
Tm	0.01	0.008	0.008	0.0051	0.01	2.5	1.3	1.3
Yb	0.087	0.058	0.07	0.08	0.082	1.8	2.2	1.6
Lu	0.028	0.014	0.022	0.02	02026	0.23	0.24	0.18
Hf				0.012		1.3		

Phase	Plag-1	Plag-1	Plag-3a	Plag-3b	Plag-4a	Plag-4a1	Herc-1	Herc-1b
Locus	I-core	I-core	I-mantle	I-mantle	I-mantle	I-mantle	I-mantle	I-mantle
Element								
Li	0.016	0.027	0.081	0.73	0.015	0.021	0.0033	0.206
Be	0.19	0.12					0.077	0.058
B	0.79	0.67	0.51	0.74	0.58	0.6	0.25	0.23
Na	34170	19900	2914	20060	6120	5740	119	10460
Mg	153	197	1210	3430	7960	1690	74520	65900
A1	152200	165800	255100	214700	301400	250600	317500	29810
Si	233499	233499	233499	233499	233499	233499	237	26300
P	66	47	24	24	26	31	0.89	5.7
K	2330	990	120	1080	290	290	570	570
Ca	71200	89900	163400	133800	151300	148300	151	7810
Sc			26	22	27	34	0.64	0.92
Ti	7.6	4	132	192	560	68	774	2070
V	2.8	1.9	3.6	6.3	25	4.3	226	2.6
Cr	2.3	0.55	4.8	13.4	72	11	681	656
Mn	71	87	106	78	213	115	1340	1270
Co	6.2	9.2	11	9.2	329	48	2870	2700
Rb	2.5	0.9	0.63	2.4	1.7	0.9	45	19
Sr	126	116	120	122	124	116	0.79	22
Y	0.13	0.14	0.8	1.1	0.58	0.44	0.54	0.92
Zr	0.34	0.056	1.4	9.4	3.6	1.3	9.4	17

(Continued)

APPENDIX. (Continued).

Phase	Plag-1	Plag-2	Plag-3a	Plag-3b	Plag-4a	Plag-4a1	Herc-1	Herc-1b
Locus	I-core	I-core	I-mantle	I-mantle	I-mantle	I-mantle	I-mantle	I-mantle
Nb	0.007	0.004	0.058	0.3	1.7	0.16	2.8	14.5
Ba	29	18	11	26	14	13	8.2	18
La	4.3	4.9	14	11	19	16	2.8	3.9
Ce	8.9	11	31	26	30	25	4.9	6.5
Pr	0.76	1.3	4	3.1	3.1	2.4	0.55	0.78
Nd	3.1	5	16	13	12	9.4	2.7	4
Sm	0.32	0.8	3.2	2.6	1.5	1.2	0.5	0.95
Eu	0.28	0.28	0.42	0.33	0.3	0.29	0.011	0.055
Gd		0.18	1.1	1.4	0.7	0.9	0.29	0.55
Tb	0.013	0.01	0.18	0.15			0.07	0.08
Dy	0.041	0.09	0.79	0.9	0.39	0.26	0.3	0.42
Ho	0.13	0.009	0.067	0.07	0.039	0.02	0.038	0.06
Er	0.04	0.036	0.18	0.16	0.18	0.13	0.1	0.14
Tm	0.008	0.005	0.15	0.21	0.24	0.11	0.01	0.14
Yb	0.015	0.026	0.15	0.11	0.12		0.07	0.08
Lu		0.004			0.032	0.016		
Hf							0.22	

Phase	Herc-2a	Herc-2b	Mt-1.2	Mt-1.3	Mt-1.4	Mt-1.5	Mt-1	Mt-2
Locus	I-mantle	I-mantle	Chon	Chon	Chon	Chon	I-mantle	I-mantle
Element								
Li	0.0009	0.012	0.028	2.15	4.8	4.5	0.059	0.17
Be	0.059	0.062					0.022	0.0011
B	0.17	0.22					0.49	0.07
Na	41.3	796	19.5	43130	106810	99140	2456	33.5
Mg	66100	60100	2205	7920	17920	16330	6540	1470
A1	310200	310000	15060	13800	12800	8550	29900	8640
Si	2640	6290	31	73130	208900	202300	47800	400
P	0.39	0.96	553	1390	1870	1010	14	15
K	8.1	60	3.3	1710	4010	3740	383	72
Ca	1430	4060	1300	12920	30200	26200	35500	780
Sc	0.69	1.2	5.1	6.3	7.8	5.8	23	10
Ti	468	2410	212900	21300	13650	5770	16030	10930
V	203	198	2660	2160	1600	880	2100	2210
Cr	575	607	94890	74870	54730	30160	635	629
Mn	1150	1210	745	682	500	261	513	247
Co	2470	2520	73	60	49	29	335	143
Rb	16	13					6.1	0.8
Sr	1.7	5.9	0.6	47	129	118	44	1.7
Y	1.1	0.72	0.14	0.91	1.9	1.7	18	0.2
Zr	8.4	12	1.7	35	96	92	28	9
Nb	3.8	22	2.8	3.9	4.1	2.4	49	0.92
Ba	0.74	2.6	0.079	47	122	111	10	1.3
La	5.5	5.5	0.094	1.2	2.8	2.4	28	3
Ce	8.9	9.5	0.2	2.3	5.1	4.4	97	5
Pr	0.92	1.2					18	0.36
Nd	4.1	4.7	0.14	0.96	2	1.7	128	2
Sm	0.87	0.87					53	0.53
Eu	0.018	0.034	0.007	0.038	0.054	0.47		
Gd	0.47	0.4					23	0.19
Th	0.066	0.04		0.024	0.02	0.032	5	0.021
Dy	0.41	0.46	0.03	0.16	0.32	0.33	27	0.17
Ho	0.047	0.064	0.006	0.036	0.078	0.078	2.6	0.26
Er	0.15	0.12	0.015	0.12	0.24	0.23	4.5	0.06
Tm	0.16	0.16	0.003	0.017	0.04	0.037	7.3	0.06
Yb	0.06	0.1	0.016				2.7	0.06
Lu	0.014	0.02	0.005	0.019	0.054	0.039	0.28	0.012
Hf	0.11		0.013	0.74	1.7	1.6		

(Continued)

APPENDIX. (Continued).

Phase	Mt-3	Obsc-1	Obsc-2	Ilm-1	Ap	Cc	Cc2
Locus	Chon	I-mantle	I-mantle	I-mantle	I-core	I-core	I-core
Element							
Li	0.042	0.89	0.34	0.01	4	2.9	0.9
Be		0.25	0.23	0.006	0.078	0.04	0.0042
B	0.037	5	4.3	0.077	25	1.1	0.73
Na	19.5	22810	27750	32.3	3250	4830	355
Mg	4790	352500	35300	14840	133400	62700	1190
A1	34350	1753600	522500	18300	9530	18260	198
Si	1310	413000	485000	180	129300	86000	570
P	780	410	220	11	81800	340	370
K	1.4	2800	2550	37	3040	440	70
Ca	1780	319500	319500	94	369200	390500	390500
Sc	8	160	190	110	20	4	
Ti	25790	84850	64000	323600	116	20	10
V	3070	11660	4540	2690	9.5	1.9	0.11
Cr	88870	6680	1580	928	114	121	67
Mn	1180	8400	1790	6450	1200	790	3.2
Co	170	14740	1650	418			
Rb	1.6	116	40	1	16	8	0.11
Sr	0.92	400	380	1.8	270	240	250
Y	0.34	120	250	0.18	56	1	0.82
Zr	3.6	230	260	40	10	0.4	0.22
Nb	0.75	270	340	190	0.36		0.008
Ba	0.12	188	77	1	33	27	37
La	0.21	180	410	0.7	22	0.4	0.14
Ce	0.58	640	1380	1.6	68	1.3	0.27
Pr	0.08	120	260	0.31	10		0.04
Nd	0.33	780	1680	1.1	54	0.9	0.35
Sm	0.04	320	690	0.2	14		0.08
Eu	0.015	4	4		2.5		0.04
Gd		100	250	0.15	10		0.09
Tb		22	52	0.02	1.7		
Dy	0.08	150	340	0.16	10.2		0.13
Ho	0.02	15	26	0.028	2.2		0.026
Er	0.07	29	47	0.08	5.1		0.08
Tm	0.011	41	113	0.07	1.1		0.025
Yb	0.03	21	38		4.1		0.13
Lu		4	6		0.67		0.036
Hf	0.21			1.2			

01: olivine; Cpx: Ca-rich pyroxene; Plag: plagioclase; Herc: hercynite; Mt: magnetite; Obsc: obscurite; Ilm: ilmenite; Ap: apatite; Cc: Ca carbonate.